Inorg. Chem. **2007**, *46*, 2432–2445

Synthesis of Pd Complexes Combined with Photosensitizing of a Ruthenium(II) Polypyridyl Moiety through a Series of Substituted Bipyrimidine Bridges. Substituent Effect of the Bridging Ligand on the Photocatalytic Dimerization of α-Methylstyrene

Akiko Inagaki,* Shinichi Yatsuda, Shinichi Edure, Akiko Suzuki, Takeshi Takahashi, and Munetaka Akita*

Chemical Resources Laboratory, Tokyo Institute of Technology, R1-27, 4259 Nagatsuta, Midori-ku, Yokohama 226-8503, Japan

Received July 13, 2006

Mononuclear ruthenium complexes and dinuclear Ru···Pd complexes having a series of 2,2′-bipyrimidine ligands, $[(bpy)_2Ru(\mathbf{L}_n)]^{2+}$ [$\mathbf{L}_n$ = 2,2′-bipyrimidine (**L1**), 5,5′-dimethyl-2,2′-bipyrimidine (**L2**), 5,5′-dibromo-2,2′-bipyrimidine (**L3**), 4,4′-dimethyl-2,2′-bipyrimidine (**L4**), and 4,4′,6,6′-tetramethyl- 2,2′-bipyrimidine (**L5**)] and $[(bpy)_2Ru(\mathbf{L}_n)PdL]^{m+}$ [$\mathbf{L}_n$ = **L1**–**L3**; PdL = PdMeCl (m = 2) and PdMe(solvent) (m = 3)], are prepared, and the obtained complexes are characterized by means of spectroscopic and crystallographic methods. Introduction of the substituents on the bipyrimidine ligands led to the substantial differences in their electrochemical and photophysical properties. Density functional theory calculations have been performed to understand the substituent effect on the ground-state molecular orbital energy level. Reactivity studies on the catalytic dimerization of α-methylstyrene revealed that the Pd complex having a Br-substituted bipyrimidine ligand were much more active than those of the corresponding Pd complexes having methyl-substituted or nonsubstituted bipyrimidine ligands.

Introduction

A significant research effort has been devoted to the synthesis and photophysical characterization of supramolecular systems capable of performing photoinduced energy or electron transfer.[1] These systems consist of molecular components with definite individual functions and bridging ligands that can link the components in an appropriate structure. Ruthenium(II) polypyridyl complexes have been widely used in a variety of systems as photoactive components because they show favorable physical properties such as long excited-state lifetimes and high luminescent efficiencies. Thus, a great number of multinuclear metal complexes containing ruthenium(II) polypyridyl moieties have been synthesized as models of the supramolecular systems in studying fundamental electron- and energy-transfer processes.[2] In spite of this situation, studies on the photochemical transformation of organic substrates using the photoactive complexes as catalysts still remain to be explored.[3,4] One of the factors is that a general synthetic method to introduce a reactive metal fragment that possesses both stability against photodecomposition and a high reactivity has not been established yet.

We have been interested in catalytic chemical transformations promoted by the sunlight, and our efforts have been directed toward preparing transition-metal complexes con-

* To whom correspondence should be addressed. E-mail: akiko_inagaki@res.titech.ac.jp (A.I.), makita@res.titech.ac.jp (M.A.).

(1) Sauvage, J.-P.; Collin, J.-P.; Chambron, J.-C.; Guillerez, S.; Balzani, V.; Barigelletti, F.; De Cola, L.; Flamigni, L. *Chem. Rev.* **1994**, *94*, 993 and references cited therein. Balzani, V.; Scandola, F. *Supramolecular Photochemistry*; Horwood: Chichester, England, 1990. Denti, G.; Serroni, S.; Campagna, S.; Ricevuto, V.; Balzani, V. *Coord. Chem. Rev.* **1991**, *111*, 227. Denti, G.; Campagna, S.; Sabatino, L.; Lerroni, S.; Ciano, M.; Balzani, V. *Inorg. Chem.* **1990**, *29*, 4750.

(2) (a) Balzani, V.; Juris, A.; Venturi, M.; Campagna, S.; Serroni, S. *Chem. Rev.* **1996**, *96*, 759 and references cited therein. (b) Schubert, U. S.; Eschbaumer, C. *Angew. Chem., Int. Ed.* **2002**, *41*, 2892. (c) Polson, M. I. J.; Hanan, G. S.; Nicholas, J. T.; Hasenknopf, B.; Thouvenot, R. *Chem. Commun.* **2004**, 1314. (d) Weldon, S.; Hammarström, L.; Mukhtar, E.; Hage, R.; Gunneweg, E.; Haasnoot, J. G.; Reedijk, J.; Browne, W. R.; Guckian, A. L.; Vos, J. G. *Inorg. Chem.* **2004**, *43*, 4471.

(3) (a) Catalytic olefin isomerization on Ru: Osawa, M.; Hoshino, M.; Wakatsuki, Y. *Angew. Chem., Int. Ed.* **2001**, *40*, 3472. (b) Stoichiometric oxidative addition on Pt: Yam, V. W.-W.; Lee, V. W.-M.; Cheung, K.-K. *Organometallics* **1997**, *16*, 2833. (c) Catalytic photoreduction on Pt: Ozawa, H.; Haga, M.; Sakai, K. *J. Am. Chem. Soc.* **2006**, *128*, 4926. (d) Catalytic photoreduction on Ni: Kimura, E.; Bu, X.; Shionoya, M.; Wada, S.; Maruyama, S. *Inorg. Chem.* **1992**, *31*, 4542. (e) Rau, S.; Schäfer, D.; Gleich, D.; Anderson, E.; Rudolph, M.; Friedrich, M.; Görls, H.; Henry, W.; Vos, J. G. Catalytic hydrogen production on Pd. *Angew. Chem. Int. Ed.* **2006**, *45*, 6215. (f) Osawa, M.; Nagai, H.; Akita, M. Pd-catalyzed Sonogashira coupling. *Dalton Trans.* **2007**, 827.

(4) Rau, S.; Walther, D.; Vos, J. G. *Dalton Trans.* **2007**, 915.

10.1021/ic0612909 CCC: $37.00
Published on Web 03/01/2007

Scheme 1

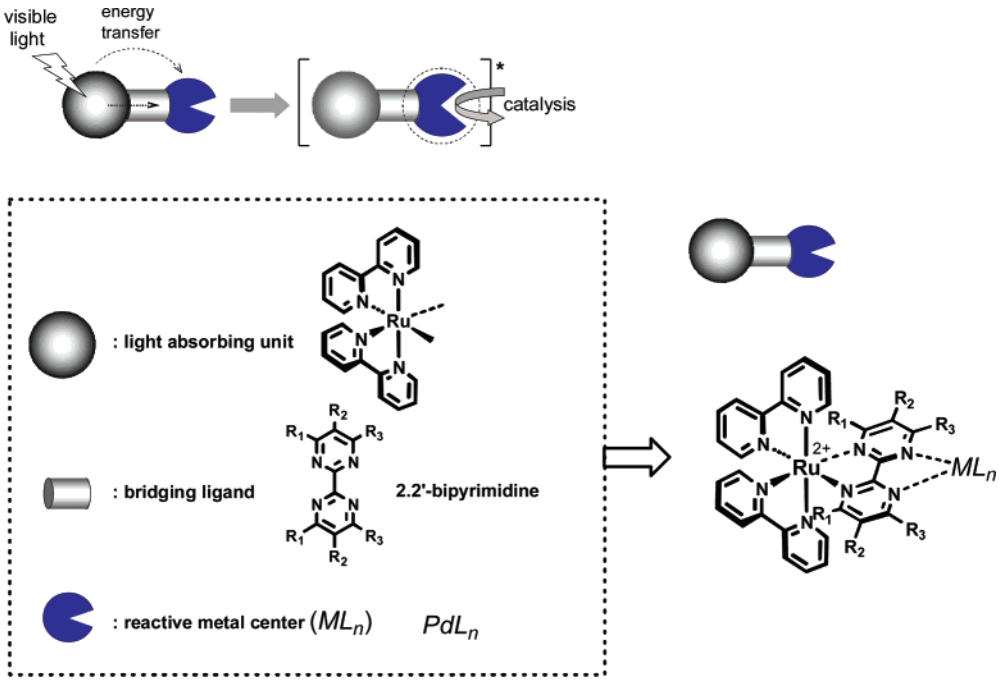

taining a visible-light-absorbing unit (Scheme 1). For the synthesis of such complexes, we chose the ruthenium(II) polypyridyl unit as the light-absorbing unit and a Pd organometallic fragment as the reaction center, and they were linked by a series of 2,2′-bipyrimidines, which are rigid π-conjugated molecules capable of connecting two units through their two bidentate coordination sites.

As a part of the early efforts, we recently reported on the synthesis of a Pd complex containing the ruthenium(II) polypyridyl moiety $[(bpy)_2Ru(bpm)PdMe(Me_2CO)](PF_6)_2$-$(BF_4)$ and its photochemical reaction with α-olefins. As a result, it was found that α-methylstyrene was selectively dimerized to yield 2,4-diphenyl-4-methyl-1-pentene by visible light irradiation (eq 1).[5] The mechanistic studies of the

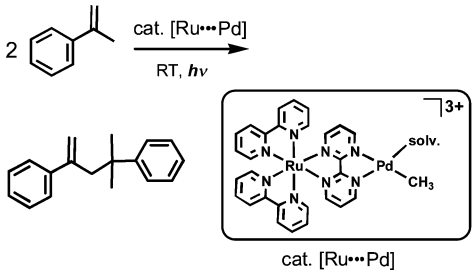

(1)

photocatalytic dimerization revealed that insertion of the second molecule, which may probably be the rate-determining step, was accelerated by visible light. It was also confirmed that the reaction was not effective by *intermolecular* sensitization but by *intramolecular* sensitization.[6] These results strongly suggested that the exciplex formation was involved in the reaction. In photoinduced energy- and electron-transfer processes, it is well-established that bridging ligands linking the photoactive unit and the acceptor play a key role in defining the efficiency of the processes.[7] At the same time, the bridging ligands give large *sterical* and *electronical* effects on the reaction site, in this case, the Pd centers. Thus, systematic studies of the complexes may lead to efficient catalytic systems capable of utilizing solar energy. As an extension of the recent work, we report herein the synthesis, characterization, electrochemistry, and photophysics of dinuclear Pd complexes with the ruthenium(II) polypyridyl moiety linked by a series of 2,2′-bipyrimidine bridging ligands together with their parent mononuclear complexes, $[(bpy)_2Ru(\mathbf{L}_n)]^{2+}$. In order to assess the substituent effect on photochemical reactions, reactivity studies on the photocatalytic dimerization of α-methylstyrene using Pd catalysts having various substituents on 2,2′-bipyrimidine are also described.

Results and Discussion

Synthesis of Mononuclear Ru Complexes. Ru complexes with bipyrimidines, $[(bpy)_2Ru(\mathbf{L2})]^{2+}$ (**2**) and $[(bpy)_2Ru$-$(\mathbf{L3})]^{2+}$ (**3**), were prepared by treating the ligands (**L2** = 5,5′-dimethyl-2,2′-bipyrimidine and **L3** = 5,5′-dibromo-2,2′-bipyrimidine) with $[(bpy)_2RuCl_2]\cdot 2H_2O$ according to the published method for the synthesis of $[(bpy)_2Ru(\mathbf{L1})]^{2+}$ (**1**; **L1** = 2,2′-bipyrimidine;[8] Scheme 2). Complex **4A** ($[(bpy)_2Ru$-

(5) Inagaki, A.; Edure, S.; Yatsuda, S.; Akita, M. *Chem. Commun.* **2005**, 5468.

(6) The reaction did not proceed when a 1:1 mixture of $[(bpy)_3Ru](PF_6)_2$ and $[(bpy)PdMe(Me_2CO)]BF_4$ was used as a catalyst.

(7) (a) Sahai, R.; Rillema, D. P.; Shaver, R.; Van Wallendael, S.; Jackman, D. C.; Boldaji, M. *Inorg. Chem.* **1989**, *28*, 1022. (b) Tapolsky, G.; Duesing, R.; Meyer, T. J. *Inorg. Chem.* **1990**, *29*, 2285. (c) Treadway, J. A.; Loeb, B.; Lopez, R.; Anderson, P. A.; Keene, F. R.; Meyer, T. J. *Inorg. Chem.* **1996**, *35*, 2242. (d) Riesgo, E.; Hu, Y.-Z.; Bouvier, F.; Thummerl, R. P. *Inorg. Chem.* **2001**, *40*, 2541. (e) Cola, D. L.; Balzani, V.; Barigelletti, F.; Flamigni, L.; Belser, P.; von Zelewsky, A.; Frank, M.; Vögtle, F. *Inorg. Chem.* **1993**, *32*, 5228. (f) Schlicke, B.; Belser, P.; Cola, D. L.; Sabbioni, E.; Balzani, V. *J. Am. Chem. Soc.* **1999**, *121*, 4207.

Scheme 2

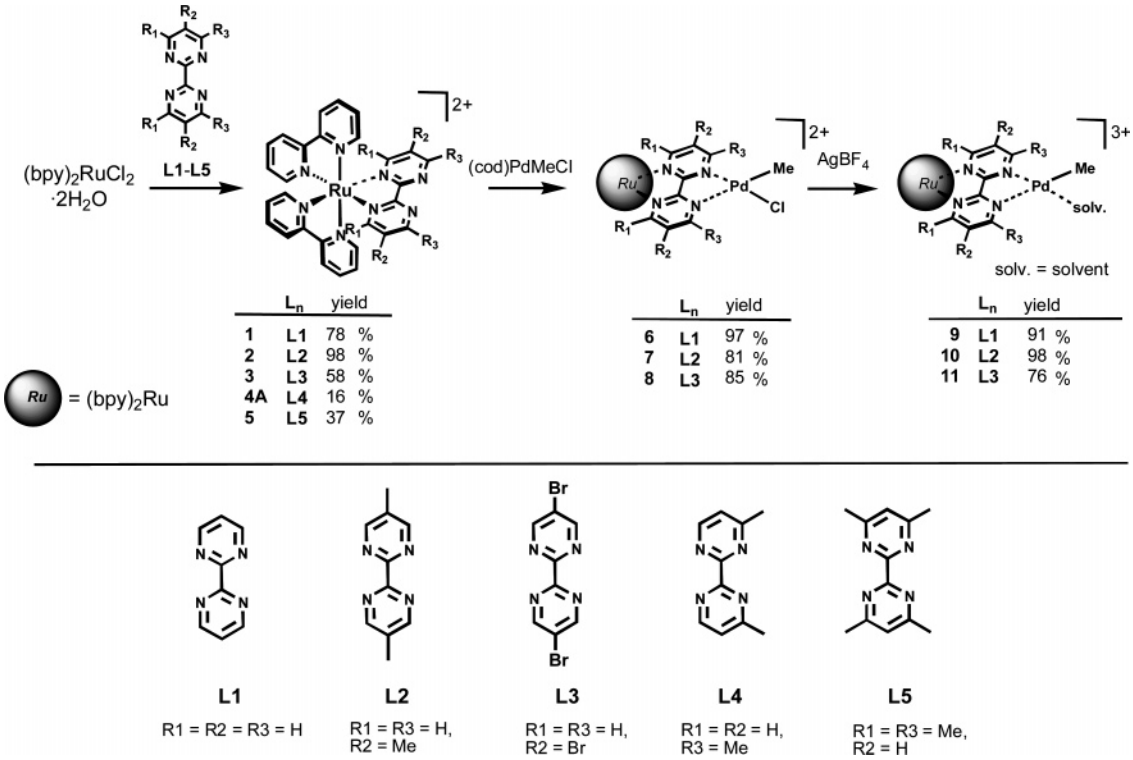

Chart 1. Structures of **4A** and **4B**

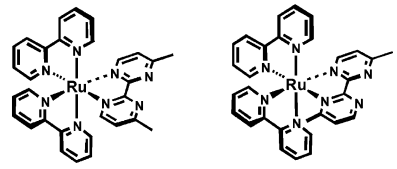

(**L4**$^{\mathbf{A}}$)]$^{2+}$) was synthesized under similar conditions with a modified purification procedure. Reaction of 4,4′-dimethylbipyrimidine (**L4**) gave a mixture of the regioisomers [(bpy)$_2$Ru(**L4**$^{\mathbf{A}}$)]$^{2+}$ (**4A**) and [(bpy)$_2$Ru(**L4**$^{\mathbf{B}}$)]$^{2+}$ (**4B**) (Chart 1), which were separated by chromatography as described in the Experimental Section.[9,10] The tetramethylbipyrimidine complex [(bpy)$_2$Ru(**L5**)]$^{2+}$ (**5**) was synthesized by treating 4,4′,6,6′-tetramethylbipyrimidine (**L5**) with the acetone complex [(bpy)$_2$Ru(Me$_2$CO)$_2$]$^{2+}$ in refluxing EtOH. It should be noted that, because all of the mono- and dinuclear complexes having the [(bpy)$_2$Ru(**L**$_n$)]$^{2+}$ (**L**$_n$ = **L1**−**L5**) moiety are chiral, they were obtained as racemates with the presented procedures.

Synthesis of Ru(L$_n$)Pd Dinuclear Complexes. The Ru···Pd dinuclear complexes [(bpy)$_2$Ru(**L**$_n$)PdMeCl]$^{2+}$ (***n*** = 1−3, **6**−**8**) were synthesized by treating the mononuclear Pd precursor, [(cod)PdMeCl]BF$_4$, with [(bpy)$_2$Ru(**L**$_n$)]$^{2+}$ (***n*** = 1−3, **1**−**3**). The corresponding solvated complexes [(bpy)$_2$Ru(**L**$_n$)PdMe(Me$_2$CO)]$^{3+}$ (***n*** = 1−3, **9**−**11**) were readily prepared by Cl$^-$ abstraction of **6**−**8** with AgBF$_4$ (Scheme 2).[4] Pd complexes having 4,4′-substituted bipyrimidine ligands (**L4** and **L5**) did not form probably because of the large steric repulsion among the substituents and the Pd center. To be noted, all of the related Rh complexes having **L1**−**L5** bridging ligands were formed in the reaction of **1**−**5** with the Rh precursor in high yields (vide infra). All of the dinuclear Ru···Pd complexes **6**−**11** were soluble in CH$_3$CN, acetone, and CH$_3$NO$_2$ and were stable for several days under the ambient light and temperature conditions.

NMR Spectroscopy. All of the mono- and dinuclear Ru complexes were unambiguously characterized on the basis of ^{1}H and ^{13}C NMR and electrospray ionization mass spectrometry (ESI-MS) spectra. The assignments of ^{1}H and ^{13}C NMR signals for **2**−**5** are based on the data of [(bpy)$_2$Ru(bpm)](PF$_6$)$_2$ assigned with 2D COSY and ^{1}H−^{13}C COSY techniques by Guadalupe et al.[7] The assignments for the dinuclear complexes **6**−**11** were made on the basis of those of the corresponding mononuclear complexes **1**−**3**.

The aromatic signals for **1**−**3** and [(bpy)$_2$Ru(**L3**)PdMe(Me$_2$CO)]$^{3+}$ (**11**) are displayed in Figure 1a. The protons on the bipyrimidine ring (H4 and H6) could be easily recognized by their coupling constants, and their assignments were made as compared with the ^{1}H NMR data of the corresponding free ligands and **1**. For all of the complexes, the signals for H6 are shifted upfield by nearly 1 ppm from those of the free ligands probably because of the ring current effect of the bipyridine ring, while the chemical shift change for H4 was very small. When the signals of **11** are compared with those of **3**, one of the two sets of signals of the bipyridine rings has been broadened (labeled as *b* in Figure 1a) in addition to the H4 and H6 signals of the bipyrimidine ring.

(8) Ji, A.; Huang, S. D.; Guadalupe, A. R. *Inorg. Chim. Acta* **2000**, *305*, 127.

(9) The synthesis and physical properties of the 4,4′-dimethylbipyrimidine complex **4** were already reported by Dose and Wilson,[9] but no spectroscopic data were provided.

(10) Dose, E. V.; Wilson, L. J. *Inorg. Chem.* **1978**, *17*, 2660.

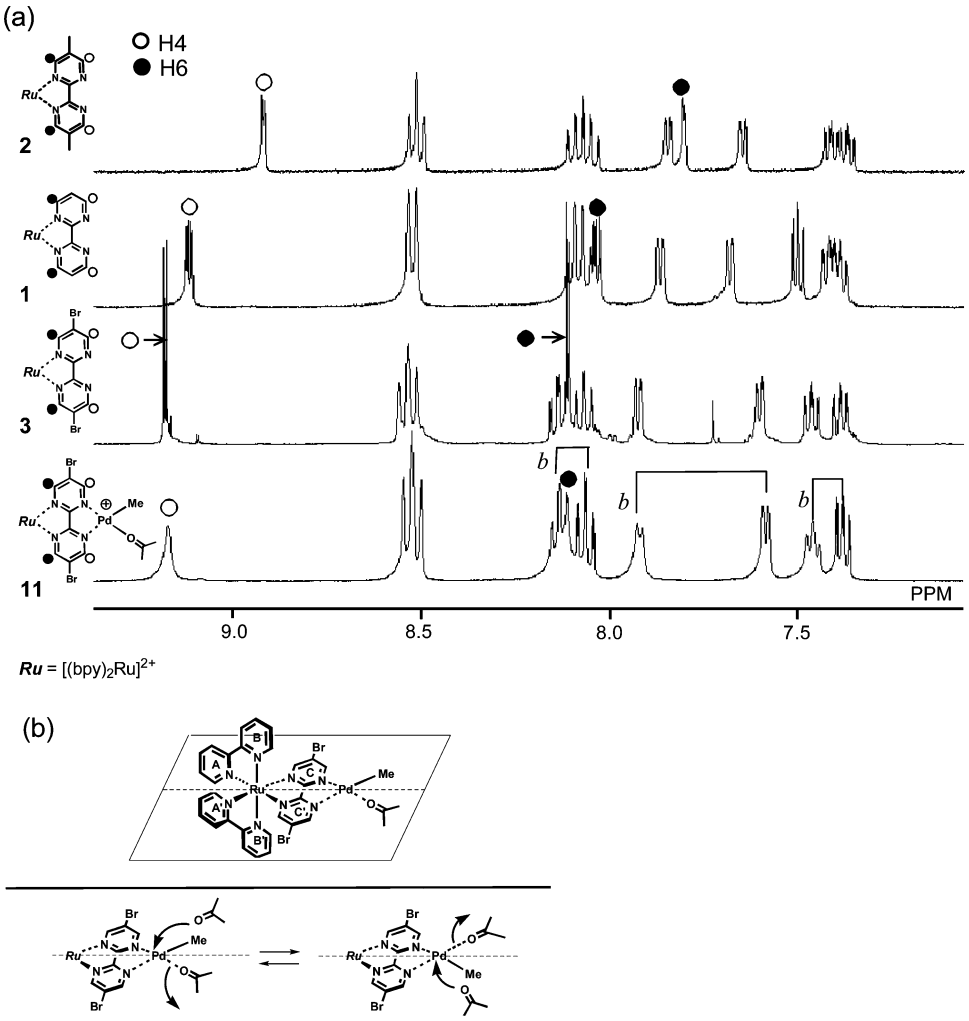

Figure 1. (a) ^{1}H NMR spectra of **2**, **1**, **3**, and **11** (top to bottom). Filled circle; 6H. Open circle: 4H. The broadened signals in the spectra of **11** are labeled as *b*. (b) Related fluxional behavior of **11**.

Chart 2. Schematic Diagram of Planes I−IV

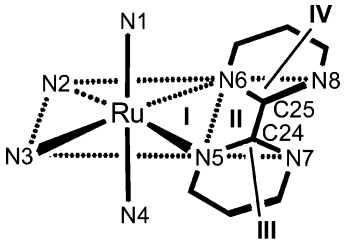

The broadened signals and the apparent symmetrical structure of **11** on the NMR time scale may be due to the solvent ligand substitution via an associative pathway (Figure 1b), resulting in the coalescence of the unequivalent proton signals on the ring A/A′ and C/C′.

Structures. ORTEP diagrams of the cationic parts of the mononuclear complexes **2**−**5** and the dinuclear Ru···Pd complex **6** are shown in Figure 2, crystal and data collection parameters are given in Table 1, and representative structural parameters are summarized in Table 2.[11] κ^2 chelations of the two bipyridine and one bipyrimidine ligands led to the slightly distorted octahedral geometry. The Ru−N bond distances are within the range normally associated with the related complexes.[7,12] In order to estimate the bending of the bipyrimidine ligand from the basal N2−N3−N5−N6 plane of the octahedron as well as the twisting of the two pyrimidine rings, we defined four planes I−IV (Chart 2)[13] and the calculated dihedral angles (∠I−II, ∠III−IV) are shown in Table 2. Both angles for the mononuclear complexes **2**−**4** are relatively small or comparable to those of **1**, showing that the substitution at 5,5′ or 4,4′ positions of the bipyrimidine ring does not cause significant sterical repulsion with the other bipyridine rings or between the two pyrimidine rings. In contrast to the disubstituted bipyrimidine complexes, the angle (∠I−II) of the Ru complex with the tetrasubstituted bipyrimidine **L5** is substantially large. The large angle originates from the bending on the N5−N6 axis to alleviate unfavorable repulsions between the "internal" methyl groups (C29 and C31) and the bipyridine ligands.

(11) Three BF_4 anions were included in the single crystal of **3** although **3** is a dicationic complex. It may be possible that Br was protonated to have a BF_4 anion as its counterion.

(12) (a) Ferrari, M. B.; Fava, G. G.; Pelosi, G.; Predieri, G.; Vignali, C.; Denti, G.; Serroni, S. *Inorg. Chim. Acta* **1998**, *275*−*276*, 320. (b) Fletcher, N. C.; Junk, P. C.; Reitsma, D. A.; Keene, F. R. *J. Chem. Soc., Dalton Trans.* **1998**, 133.

(13) Plane I: Ru−N5−N6. Plane II: N5−C24−C25−N6. Plane III: N5−C24−N7. Plane IV: N6−C25−N8.

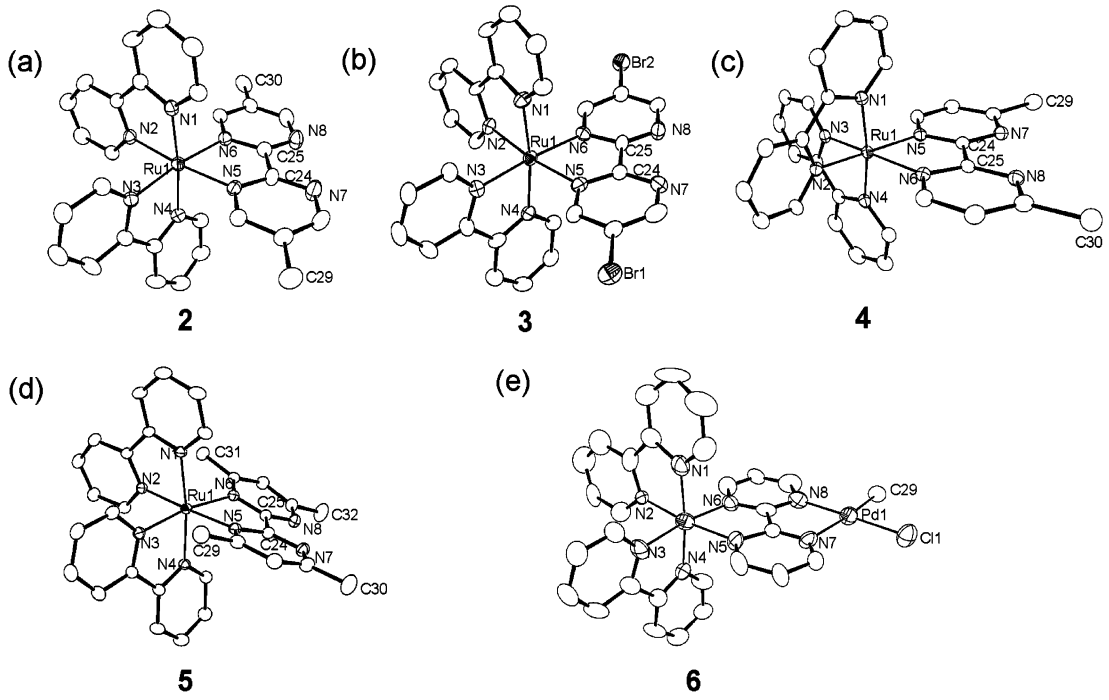

Figure 2. ORTEP drawings of the cationic parts of (a) **2**, (b) **3**, (c) **4A**, (d) **5**, and (e) **6**.

Table 1. Crystallographic Data for **2**−**6**

	2	**3**	**4A**	**5**	**6**
formula	$C_{32}H_{29}B_2F_8N_9Ru$	$C_{29}H_{24}B_3F_{12}N_9Br_2O_2Ru$	$C_{33}H_{32}F_{12}N_8P_2ORu$	$C_{32}H_{30}F_{12}N_8P_2Ru$	$C_{31}H_{31}ClF_{12}N_{10}O_4P_2PdRu$
formula weight	814.33	1051.9	947.68	917.65	1140.52
cryst syst	triclinic	triclinic	monoclinic	orthorhombic	triclinic
space group	$P\bar{1}$ (No. 2)	$P\bar{1}$ (No. 2)	$P2_1/a$ (No. 14)	*Pbca* (No. 61)	$P\bar{1}$ (No. 2)
a/Å	11.0233(15)	11.034(6)	13.247(3)	18.185(3)	9.526(7)
b/Å	12.527(3)	12.604(7)	23.613(6)	13.904(4)	11.290(9)
c/Å	13.660(3)	13.510(5)	12.127(3)	28.103(9)	20.075(16)
α/deg	108.132(5)	105.67(3)	90	90	100.42(3)
β/deg	100.310(9)	98.47(3)	99.452(18)	90	102.89(3)
γ/deg	98.311(11)	100.79(1)	90	90	96.73(3)
V/Å^3	1722.7(6)	1737(1)	3741.9(15)	7105.8(3)	2042(3)
Z	2	2	4	8	2
d_{calcd}/g cm^{-3}	1.570	2.010	1.682	1.716	1.656
T/K	−60	−60	−160	−60	−60
radiation	Mo Kα ($\lambda = 0.71069$ Å)	Mo Kα ($\lambda = 0.71069$ Å)	Mo Kα ($\lambda = 0.71069$ Å)	Mo Kα ($\lambda = 0.71069$ Å)	Mo Kα ($\lambda = 0.71069$ Å)
μ/cm^{-1}	5.37	5.28	6.06	6.33	10.41
diffractometer	Rigaku RAXIS IV	Rigaku RAXIS IV	Rigaku AFC7R	Rigaku RAXIS IV	Rigaku RAXIS IV
max 2*θ*/deg	55.0	55.0	55.0	55.0	55.0
reflns collcd	14119	11642	9014	51766	10980
indep reflns	7173 [*R*(int) = 0.0738]	7720 [*R*(int) = 0.0903]	8648 [*R*(int) = 0.0626]	8139 [*R*(int) = 0.0651]	7205 [*R*(int) = 0.144]
no. of param refined	527	560	612	615	572
R1 ($I > 2\sigma$)	5.52	9.27	5.11	4.64	6.87
wR2 ($I > 2\sigma$)	13.37	27.42	13.92	11.92	11.87
GOF	1.032	1.005	1.031	1.041	0.765

The X-ray crystal structures of the dinuclear Ru···Pd complexes **6** and **9** have also been determined, of which the structure of **9** (solv. = CH_3CN) was described previously.[4] The structure of the Ru−Pd dinuclear complex **6** is quite similar to that of the MeCN-coordinated cationic species **9**.[4] The bond distances and angles around the Ru atom are comparable to those found for the mononuclear Ru complexes.[12] Substantial elongation of one of the Pd−N bonds [Pd1−N7 = 2.169(12) Å vs Pd1−N8 = 2.047(13) Å] was probably due to the larger trans effect of the methyl group. The dihedral angles of **6** (∠I−II = 2.82°; ∠III−IV = 2.73°) were also comparable to those of the corresponding mononuclear complex **1** (∠I−II = 1.88°; ∠III−IV = 3.33°). These structural features of the dinuclear complex **6** clearly demonstrate that introduction of the second metal fragment does not cause any significant structural distortion to the light-absorbing Ru unit in the case for dinuclear complexes having nonsubstituted bipyrimidine (**L1**) as a bridging ligand.[14]

Electrochemistry. The redox potentials for the obtained

Table 2. Selected Bond Distances (Å) and Angles (deg) for **2**−**6** and **9**

	2	3	4A	5	6	9[a]
			Bond Distances (Å)			
Ru1−N1	2.074(4)	2.102(9)	2.064(3)	2.080(2)	2.021(14)	2.092(9)
Ru1−N2	2.063(4)	2.076(9)	2.063(3)	2.069(2)	2.025(15)	2.075(9)
Ru1−N3	2.077(3)	2.083(9)	2.065(3)	2.052(2)	2.056(12)	2.077(9)
Ru1−N4	2.062(4)	2.093(9)	2.062(3)	2.069(2)	2.007(12)	2.064(9)
Ru1−N5	2.072(4)	2.056(8)	2.062(3)	2.110(2)	2.016(12)	2.069(8)
Ru1−N6	2.075(3)	2.097(9)	2.068(3)	2.113(2)	2.069(11)	2.073(9)
			Bond Angles (deg)			
N1−Ru1−N2	78.51(15)	78.8(4)	78.49(13)	78.34(9)	79.7(6)	78.3(4)
N3−Ru1−N4	78.35(14)	78.8(4)	78.74(12)	78.68(9)	78.1(6)	79.4(4)
N5−Ru1−N6	78.78(14)	78.2(4)	78.46(11)	78.13(8)	77.4(5)	79.1(3)
			Plane Angles (deg)			
I−II	4.39	1.85	0.11	19.09	2.82	4.71
III−IV	1.90	0.31	3.40	6.53	2.73	3.87

[a] From ref 4.

Table 3. Redox Properties[a]

	$E_{1/2}$				
	$Ru^{II/III}$	$L^{0/1-}$	$bpm^{1-/2-}$	$L^{0/1-}$	$L^{0/1-}$
$[(bpy)_3Ru](BF_4)_2$	0.88 (55)			−1.74 (62)	−1.93 (54)
$[(bpy)_2Ru(\mathbf{L1})](BF_4)_2$ (**1**)	1.00 (68)	−1.40 (90)		−1.85 (91)	−2.14 (90)
$[(bpy)_2Ru(\mathbf{L2})](BF_4)_2$ (**2**)	0.96 (82)	−1.57 (66)		−1.87 (70)	−2.09 (76)
$[(bpy)_2Ru(\mathbf{L3})](BF_4)_2$ (**3**)	1.08 (80)	−1.21 (86)		−1.72 (irr)	−1.87 (90)
$[(bpy)_2Ru(\mathbf{L4})](BF_4)_2$ (**4**)	0.94 (64)	−1.48 (62)		−1.86 (66)	−2.09 (72)
$[(bpy)_2Ru(\mathbf{L5})](BF_4)_2$ (**5**)	0.97 (82)	−1.54 (64)		−1.89 (66)	−2.09 (72)
$[(bpy)_2Ru(\mathbf{L1})PdMeCl](BF_4)_2$ (**6**)	1.26 (66)	−0.93 (68)	−1.61 (66)	−1.94 (64)	−2.18 (71)
$[(bpy)_2Ru(\mathbf{L2})PdMeCl](BF_4)_2$ (**7**)	1.19 (80)	−1.09 (66)	−1.72 (62)	−1.95 (66)	−2.18 (74)
$[(bpy)_2Ru(\mathbf{L3})PdMeCl](BF_4)_2$ (**8**)		−0.64 (irr)	−1.66 (irr)	−1.89 (irr)	−2.17 (irr)
$[(bpy)_2Ru(\mathbf{L1})PdMe(Me_2CO)](BF_4)_3$ (**9**)	1.26 (100)	−0.85 (126)	−1.54 (64)	−1.85 (112)	−2.16 (122)
$[(bpy)_2Ru(\mathbf{L2})PdMe(Me_2CO)](BF_4)_3$ (**10**)	1.21 (72)	−1.08 (72)	−1.67 (irr)	−1.96 (irr)	−2.15 (irr)

[a] Measurements were carried out in CH_3CN with 0.1 M TBAP, V vs $E(Fc/Fc^+)$. The numbers in parentheses are the differences (mV) between the anodic and cathodic waves.

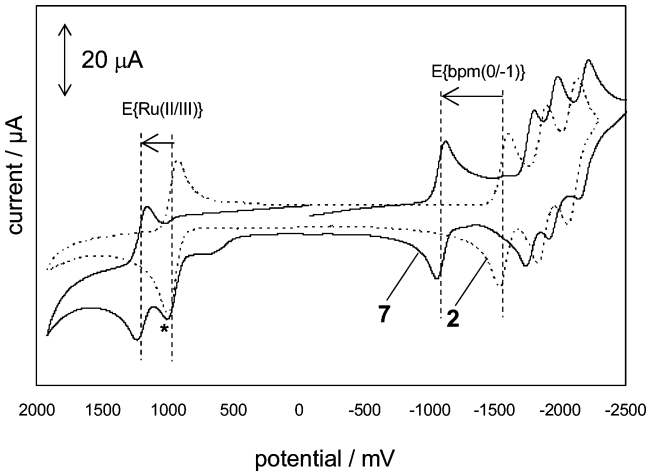

Figure 3. CVs of **2** and **7** in a CH_3CN solution: dotted line, **2**; solid line, **7**. The asterisk indicates a redox wave of the mononuclear fragment **2** formed in the CV measurement of **7**.

complexes are summarized in Table 3,[15] and cyclic voltammogram (CV) spectra of **2** and $[(bpy)_2Ru(\mathbf{L2})PdMeCl]^{2+}$ (**7**) are shown in Figure 3. In the CVs of the mononuclear complexes **1**−**5**, the single quasi-reversible waves in the anodic region are assigned to a metal-centered oxidation process ($Ru^{II/III}$) and the three one-electron redox waves in the cathodic region are assigned to the bipyrimidine- and bipyridine-centered reduction processes.[6a,16] Introduction of electron-withdrawing or -donating groups to the bipyrimidine ligand causes shifts by ca. 0.2 V to the positive or negative side, respectively, with respect to **1**. The dinuclear Ru···Pd complexes showed four cathodic redox waves that are assigned to the following redox processes: $bpm^{0/1-}$ (ca. −1.0 V), $bpm^{1-/2-}$(ca. −1.5 V), and $bpy^{0/1-}$ (ca. −1.8 and −2.0 V) (Figure 3).[3b,16,17] Introduction of the Pd fragment resulted in a shift of the redox potential of $bpm^{0/1-}$ to ca. −1.0 V, and thus the second reduction of the bipyrimidine ligand ($bpm^{1-/2-}$, ca. −1.5 V) can be also observed within the potential window as a result of the substantial decrease of the electron density on the bipyrimidine ligands. Owing to the instability of the Ru···Pd complexes with the **L3** ligand (**8** and **11**) under the CV measurement conditions, redox waves for **8** were observed as irreversible and only the waves of the mononuclear species **3** after fragmentation were observed in the CV spectra of **11**.[18] The difference of the bipyrimidine reduction potentials between **7** and **6** ($E\{\mathbf{L2}^{n/n-1}\}$

(14) Crystallographic studies of several dinuclear complexes with the metal fragments $[RuCp^*(OTf)]^+$, $[Rh(CO)_2]^+$, $[Ir(CO)_2]^+$, $[PdMe(MeCN)]^+$, and $[Pd(C_3H_5)]^+$ have been done by our group. The bond lengths and angles of the $[(bpy)_2Ru(bpm)]^{2+}$ unit of the dinuclear complexes are comparable to those of the mononuclear complex $[(bpy)_2Ru(bpm)]^{2+}$.

(15) Redox data for **11** are not shown in the table because **11** is electrochemically too unstable to detect peaks of the dinuclear compound.

(16) Rillema, D. P.; Allen, G.; Meyer, T. J.; Conrad, D. *Inorg. Chem.* **1983**, *22*, 1617.
(17) Milkevitch, M.; Brauns, E.; Brewer, K. J. *Inorg. Chem.* **1996**, *35*, 1737.
(18) See the Supporting Information for the spectra.

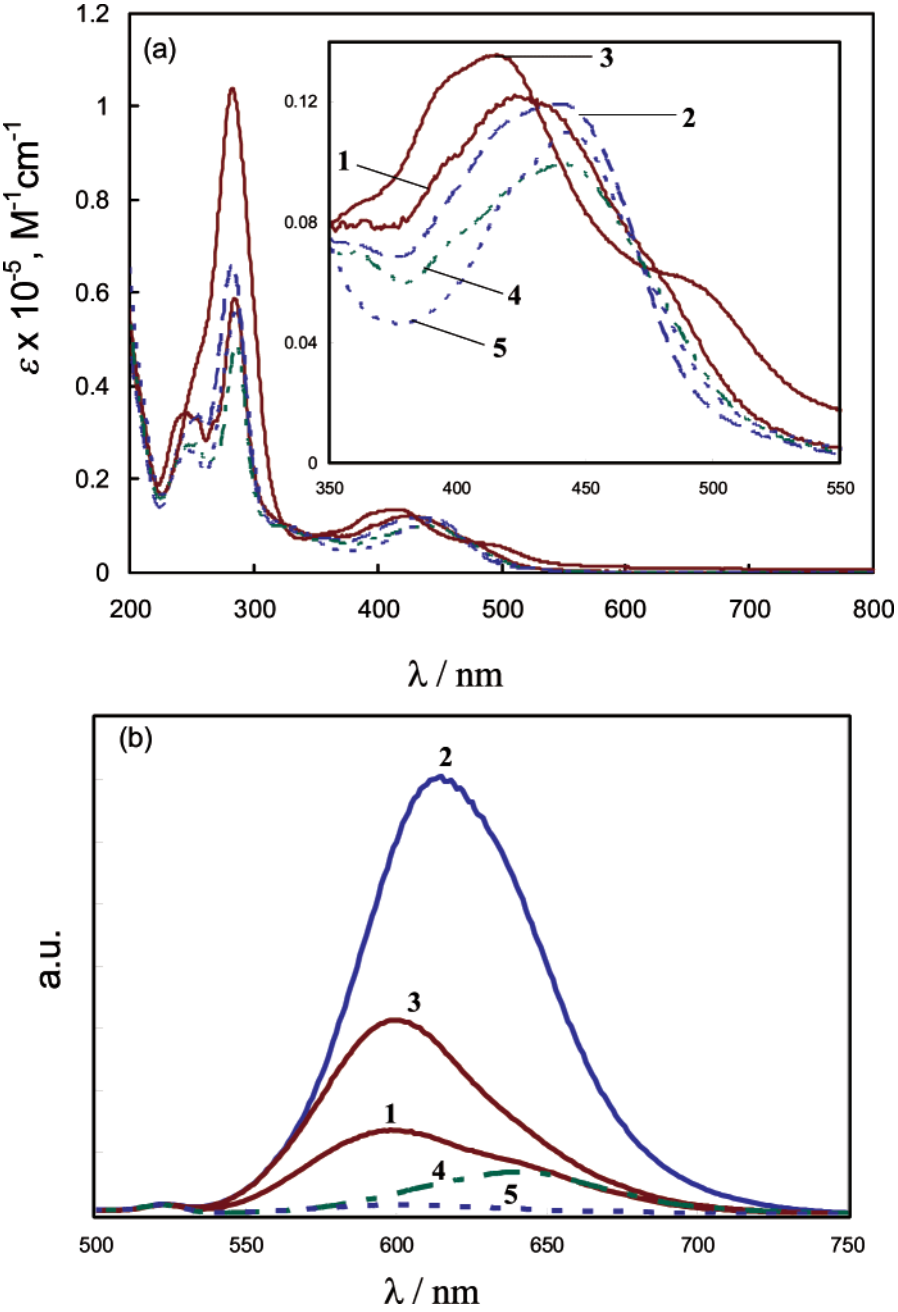

Figure 4. (a) Absorption spectra in CH_3CN for **1**−**5**. (b) Emission spectra for **1**−**5** obtained at absorbance 0.1 in CH_3CN at 293 K, with excitation at 450 nm.

$- E\{\mathbf{L1}^{n/n-1}\}$) was nearly the same as that of the corresponding mononuclear complexes of **1** and **2** ($E\{\mathbf{L2}^{0/1-}\} - E\{\mathbf{L1}^{0/1-}\}$).

Electronic Absorption. The UV−vis spectra of the complexes were recorded in deaerated acetonitrile solutions and were illustrated in Figure 4a for the mononuclear complexes **1**−**5**. The electronic absorption data for both mono- and dinuclear complexes are summarized in Table 4. These complexes exhibit intense UV absorption bands (λ_{max} = 200−300 nm) attributed to a ligand-centered $\pi \rightarrow \pi^*$ transitions and a visible absorption band (λ_{max} = 400−450 nm) attributed to a metal-to-ligand charge transfer (MLCT). The low-energy absorption bands in the visible region are overlapping with the ^{1}MLCT transitions of d(Ru) → π^*-(bpm) and d(Ru) → π^*(bpy),[16b,19] exhibiting broader bands than that of $[(bpy)_3Ru]^{2+}$. Although the differences in λ_{max} were not so significant, the low-energy absorption bands of **2**, **4**, and **5**, which possess methyl substituents on the bipyrimidine ligand, were slightly narrower than those of **1**. Complex **3** containing a dibromobipyrimidine ligand showed significantly broadened bands in the visible region to exhibit a two-peak spectrum probably due to splitting of the overlapping bipyrimidine and bipyridine absorption bands (Figure 4a, inset). These noticeable changes indicate that the π^*(bpm) energy level is stabilized upon introduction of electron-withdrawing bromo substituents whereas it is de-

(19) Ioachim, E.; Medlycott, E. A.; Hana, G. S.; Loiseau, F.; Ricevuto, V.; Campagna, S. *Inorg. Chem. Commun.* **2005**, *8*, 559.

Table 4. Electronic Absorption and Luminescence Data[a]

	absorption	luminescence at 298 K		
	λ_{max}, nm (ϵ, M^{-1} cm^{-1})	λ_{max}, nm	Φ_{rel}[b]	Φ_{rel}[c]
$[(bpy)_3Ru](PF_6)_2$[23]	452 (14000)	596	1.00	
$[(bpy)_2Ru(\mathbf{L1})](BF_4)_2$ (**1**)	423 (12000)	599	0.05	1.00
$[(bpy)_2Ru(\mathbf{L2})](BF_4)_2$ (**2**)	441 (12000)	613	0.24	4.95
$[(bpy)_2Ru(\mathbf{L3})](BF_4)_2$ (**3**)	416 (14000)	600	0.11	2.15
$[(bpy)_2Ru(\mathbf{L4})](BF_4)_2$ (**4**)	443 (10000)	642	0.02	0.44
$[(bpy)_2Ru(\mathbf{L5})](PF_6)_2$ (**5**)	446 (11000)	601	0.004	0.01
$[(bpy)_2Ru(\mathbf{L1})PdMeCl](PF_6)_2$ (**6**)	423 (14000)	599	0.13	2.65
$[(bpy)_2Ru(\mathbf{L2})PdMeCl](BF_4)_2$ (**7**)	430 (10000)	613	0.23	4.69
$[(bpy)_2Ru(\mathbf{L3})PdMeCl](BF_4)_2$ (**8**)	415 (13000)	651	0.01	0.14
$[(bpy)_2Ru(\mathbf{L1})PdMe(Me_2CO)](BF_4)_3$ (**9**)	425 (17000)	634	0.03	0.51 (0.51)[d]
$[(bpy)_2Ru(\mathbf{L2})PdMe(Me_2CO)](BF_4)_3$ (**10**)	429 (10000)	614	0.15	3.00 (0.61)[d]
$[(bpy)_2Ru(\mathbf{L3})PdMe(Me_2CO)](BF_4)_3$ (**11**)	418 (12000)	647	0.02	0.35 (0.16)[d]

[a] Measurements were carried out in deaerated CH_3CN at room temperature unless otherwise noted. [b] Relative quantum yield versus $[(bpy)_3Ru](PF_6)_2$. [c] Relative emission yield versus **1**. [d] Relative quantum yield versus the parent mononuclear complexes.

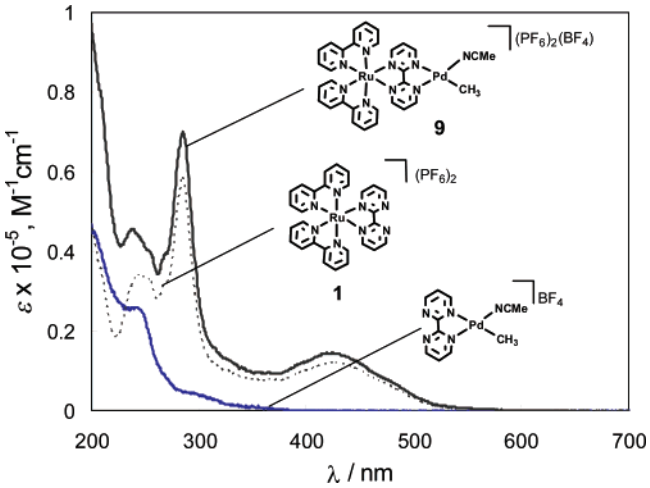

Figure 5. Absorption spectra of **9**, **1**, and [(bpm)PdMe(MeCN)]BF_4 in a deaerated CH_3CN solution.

stabilized upon introduction of electron-donating methyl substituents.

An absorption spectrum of the dinuclear Ru···Pd complex **9** is shown in Figure 5, together with those of the corresponding mononuclear components $[(bpy)_2Ru(bpm)](PF_6)_2$ and [(bpm)PdMe(MeCN)](BF_4).[20] The spectrum of **9** exhibited a low-energy absorption band at 420 nm (λ_{max} = 424 nm) due to the incorporation of a ruthenium(II) polypyridyl moiety. Other dinuclear Ru···Pd complexes **10** and **11** also contained the broad absorption in the visible region, and their spectra were very similar to those of the parent mononuclear complexes **2** and **3**, respectively. The spectra for all of the dinuclear Ru···Pd complexes are presented in the Supporting Information. It should be noted that the CV data in Table 3 indicate the consequence of Pd coordination on the reduction potentials of the bipyrimidine ligand, while almost no change is observed in the absorption bands in the visible-wavelength region. This is in contrast to the shift to lower energy in the d(Ru) → π*(bpm) transition band reported in the homo- and heterobimetallic complexes $[(bpy)_2Ru(bpm)Ru(bpy)_2]^{4+}$ [21] and $[(bpy)_2Ru(bpm)PdCl_2]^{2+}$.[3c] We still do not know what is responsible for the lack of correlation, but one possibility is that the spectroscopic orbitals may be different from the redox orbitals. We are studying the physical properties of the series of complexes to understand this further.

Table 5. Calculated and Experimental Selected Bond Lengths and Angles[a]

complex	M−N (av.)	∠N−Ru−N[b]
$[(bpy)_3Ru]^{2+}$	2.099 [2.056][c]	78.3 [78.6][c]
$[(bpy)_2Ru(\mathbf{L1})]^{2+}$	2.098 [2.060]	78.4 [78.9]
$[(bpy)_2Ru(\mathbf{L2})]^{2+}$	2.099 [2.070]	78.4 [78.6]
$[(bpy)_2Ru(\mathbf{L3})]^{2+}$	2.098 [2.084]	78.4 [78.6]
$[(bpy)_2Ru(\mathbf{L4})]^{2+}$	2.098 [2.064]	78.3 [78.6]
$[(bpy)_2Ru(\mathbf{L5})]^{2+}$	2.116 [2.082]	78.3 [78.4]
$[(bpy)_2Ru(\mathbf{L1})PdMe(MeCN)]^{3+}$	2.105 [2.072]	78.4 [78.5]

[a] The numbers in parentheses are the corresponding bond lengths obtained from the crystallographic data. [b] Averaged intraligand angles. [c] From ref 26.

The emission spectra of mononuclear Ru complexes were recorded in deaerated acetonitrile solutions at room temperature and are depicted in Figure 4b. The spectra were acquired for solutions of equal absorbance (0.1) at the 450 nm excitation wavelength. The emission maxima and relative quantum yields are listed in Table 4. The emission originates from the lowest-lying triplet MLCT [dπ(Ru)] → π*(bpy)] or [dπ(Ru)] → π*(bpm)] in accordance with the dominant lowest unoccupied molecular orbital (LUMO) character. A remarkable increase of the emission intensity was observed for **2**, whereas the Ru complexes with **L4** and **L5** ligands showed a drastic decrease compared to that of **1**. From the theoretical study with the density functional theory (DFT) method, the LUMOs distribute predominantly on the bipyrimidine ligand for **1** but on the bipyridine ligand for **2** (vide infra). The introduction of two methyl groups raises the π*-(bpm) energy level higher than that of the π*(bpy) orbitals, which results in a radiative process similar to that of $[(bpy)_3Ru]^{3+}$. The considerably low emission intensity of $[(bpy)_2Ru(bpm)]^{2+}$ relative to **2**, **3**, and $[(bpy)_3Ru]^{2+}$ suggests the presence of a quenching process by the lone-pair electrons of the bipyrimidine N atoms. The markedly low quantum yields of **4** and **5**, which also possess methyl substituents on the bipyrimidine ligands, is probably due to the potential strain caused by repulsion of the methyl groups on the 4,4′

(20) Brookhart, M.; Wagner, M. I.; Balavoine, G. G. A.; Haddou, H. A. *J. Am. Chem. Soc.* **1994**, *116*, 3641.
(21) Kalyanasundaram, K.; Nazeeruddin, Md. K. *Inorg. Chem.* **1990**, *29*, 1888.

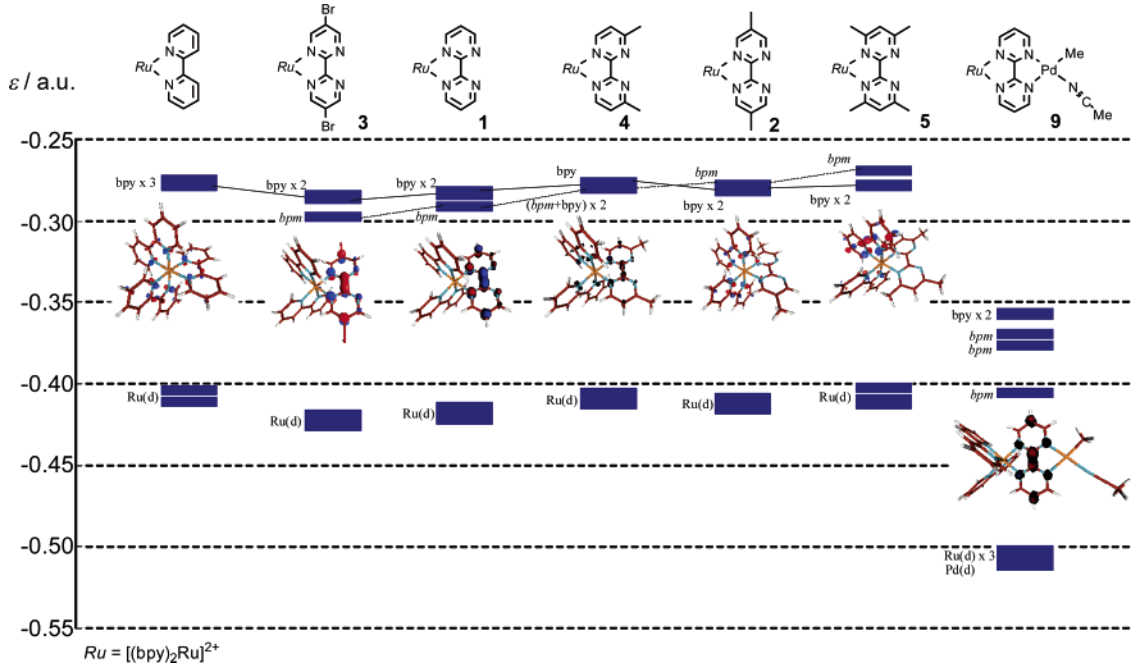

Figure 6. Energy diagram of some frontier MOs of $[(bpy)_2Ru(\mathbf{L}_n)]^{2+}$.

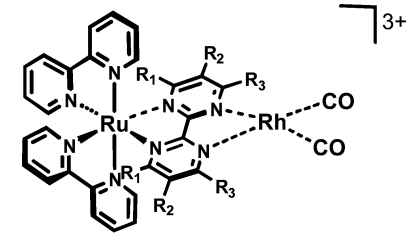

L_n	ν_{CO} (in CH_3NO_2)
L1	2093, 2023
L2	2093, 2023
L3	2093, 2023

Figure 7. ν_{CO} of the dinuclear Ru···Rh complexes.

and 6,6′ positions in addition to quenching by the lone pair.[22] From the data obtained under ambient conditions, it was not possible to assess the degree of this quenching toward each mononuclear complex, thus making it difficult to understand the series of emission data. However, there is a certain order in the relative quantum yield of the dinuclear complexes (**6**−**11**), which decrease according to their bridging ligands in the order of **L2** > **L1** > **L3**. Paying attention to the quantum yield of **9**−**11** (numbers in parentheses in Table 4), a decrease of the emission intensity indicates quenching by energy transfer from the ruthenium(II) polypyridyl moiety to the Pd center, exceeding an opposite effect (increase of the emission intensity) by loss of the free lone-pair electrons. The numbers suggest that the transfer is most efficient in the complex having an **L3** ligand.

(22) The average Mülliken charge values of the noncoordinated bipyrimidine N atoms, which have been calculated using the optimized structures obtained in the DFT calculation, were 0.518 (**3**) < 0.520 (**1**) < 0.533 (**2**) < 0.559 (**4**) < 0.561 (**5**). The data indicate the presence of a larger electronic repulsion among the free lone pairs for **4** and **5**.

(23) Synthesized and measured by our group.

DFT Study. To understand the substituent effect upon the ground-state energy level of the frontier MOs, DFT calculations of the mononuclear complexes $[(bpy)_2Ru(\mathbf{L}_n)]^{2+}$ (n = 1−5, **1**−**5**) and the dinuclear complex $[(bpy)_2Ru(\mathbf{L1})PdMe(MeCN)]^{3+}$ (**9**) have been performed with the *Gaussian 03* quantum chemistry program package.[24] Geometries of the complexes were optimized with the analytical gradient method. For geometry optimization, we used the LanL2DZ pseudopotential on Ru and Pd, the 6-31G+ split-valence basis set on N and C coordinated to Ru or Pd, 6-31G on Br, and 3-21G on the other C, H, and N atoms. The starting geometries for the optimization were taken from the X-ray crystallographic data for **1**−**5** and **9**. Geometries of the complexes were optimized without any symmetry constraint.

The calculated selective bond lengths and angles of a series of complexes and $[(bpy)_3Ru]^{2+}$ for comparison are collected in Table 5. The calculated Ru−N bond lengths were about 0.6−1.7% longer than the experimental values, but other bond lengths and angles showed good agreements. Thus, the results of the geometry optimizations by the DFT method at

(24) Frisch, M. J.; Trucks, G. W.; Schlegel, H. B.; Scuseria, G. E.; Robb, M. A.; Cheeseman, J. R.; Montgomery, J. A.; Vreven, J.; Kudin, T. K. N.; Burant, J. C.; Millam, J. M.; Iyengar, S. S.; Tomasi, J.; Barone, V.; Mennucci, B.; Cossi, M.; Scalmani, G.; Rega, N.; Petersson, G. A.; Nakatsuji, H.; Hada, M.; Ehara, M.; Toyota, K.; Fukuda, R.; Hasegawa, J.; Ishida, M.; Nakajima, T.; Honda, Y.; Kitao, O.; Nakai, H.; Klene, M.; Li, X.; Knox, J. E.; Hratchian, H. P.; Cross, J. B.; Adamo, C.; Jaramillo, J.; Gomperts, R.; Stratmann, R. E.; Yazyev, O.; Austin,A. J.; Cammi, R.; Pomelli, C.; Ochterski, J. W.; Ayala, P. Y.; Morokuma, K.; Voth, G. A.; Salvador, P.; Dannenberg, J. J.; Zakrzewski, V. G.; Dapprich, S.; Daniels, A. D.; Strain, M. C.; Farkas, O.; Malick, D. K.; Rabuck, A. D.; Raghavachari, K.; Foresman, J. B.; Ortiz, J. V.; Cui, Q.; Baboul, A. G.; Clifford, S.; Cioslowski, J.; Stefanov, B. B.; Liu, G.; Liashenko, A.; Piskorz, P.; Komaromi, I.; Martin, R. L.; Fox, D. J.; Keith, T.; Al-Laham, M. A.; Peng, C. Y.; Nanayakkara, A.; Challacombe, M.; Gill, P. M. W.; Johnson, B.; Chen, B. W.; Wong, M. W.; Gonzalez, C.; Pople, J. A. *Gaussian 03*, revision B.04; Gaussian, Inc.: Pittsburgh, PA, 2003.

Scheme 3

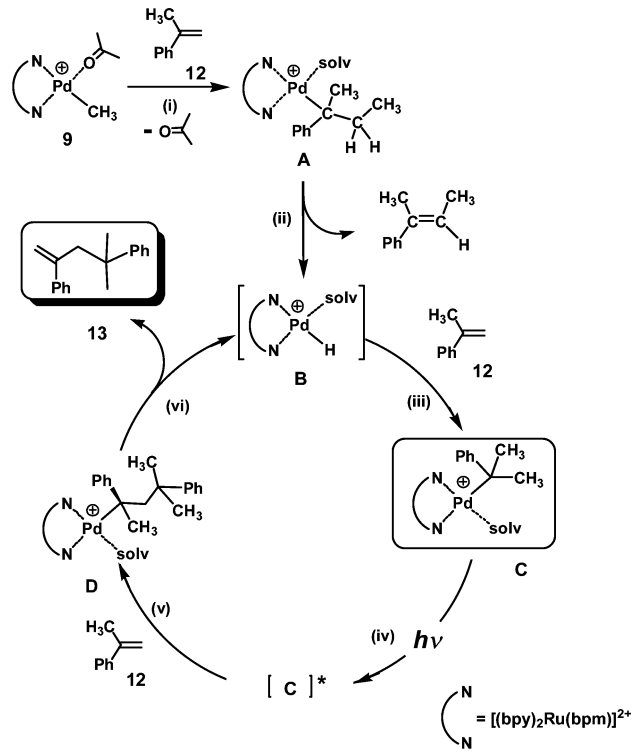

this level of calculation are reliable enough to further discuss their electronic structures. The optimized geometries and their self-consistent-field energies are provided in the Supporting Information. The calculated energies of some frontier MOs, three occupied and three unoccupied, are shown in Figure 6, together with the computed figures of the LUMOs. In the case of mononuclear complexes, the energies of the highest occupied MOs (HOMOs) and the other two occupied MOs lie near −0.4 au,[25] and these MOs are predominantly based on the Ru d orbitals. There are two unoccupied π^* orbitals that lie close to LUMO whose components distribute mainly on bipyridine and/or bipyrimidine ligands. We can see from Figure 6 that introduction of the electron-donating methyl substituents into the bipyrimidine ligands destabilizes the bipyrimidine-centered unoccupied MOs (**1** → **4** → **2** → **5**), whereas introduction of the electron-withdrawing Br substituents stabilizes the MO (**1** → **3**). Thus, introduction of the substituents led to the change in the LUMO character.

In the case of dinuclear Ru···Pd complex **9**, substantial stabilization of two of the other bipyrimidine-centered unoccupied MOs was observed. If the substituent effect in the dinuclear complexes toward the MO energy level is parallel to that in the mononuclear complexes, introduction of the Br substituents may lead to a further stabilization of the three bipyrimidine-based MOs in comparison with those of **9**. This stabilization should be advantageous to the efficient intramolecular energy transfer across the ligand bridge.

(25) 1 au (atomic unit) = 27.21 eV.
(26) Biner, M.; Bürgi, H.-B.; Ludi, A.; Röhr, C. *J. Am. Chem. Soc.* **1992**, *114*, 5197.

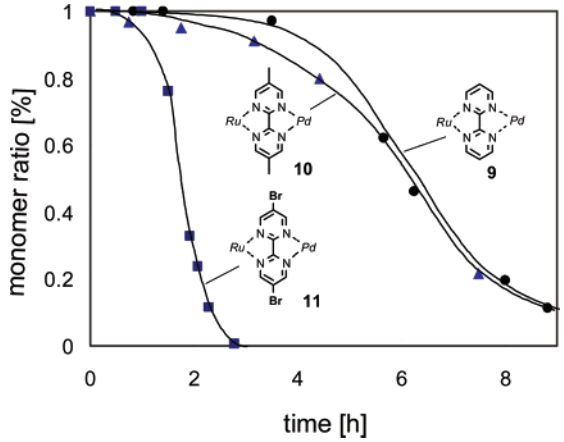

Figure 8. Consumption rate of the monomer in the reaction of **9**−**11** under irradiated conditions.

Electron Density of the Reactive Metal Centers. In order to investigate the difference of the electron density on the reactive metal centers by their substituents on the bridging ligands, wavenumbers of the corresponding rhodium carbonyl complexes[27] (ν_{CO}) are compared and listed in Figure 7. The IR spectra of a CH_3NO_2 solution of the rhodium carbonyl complexes contained two C−O stretching bands at 2093 and 2023 cm^{-1}. These numbers are comparable to those of the model complex $[(bpy)Rh(CO)_2]^+$ (ν_{CO} = 2100 and 2040 cm^{-1}), indicating that the decrease of the electron density on the Rh center is not significant. Moreover, whether the substituents on the bipyrimidine ligands are H, Me, or Br, C−O stretching bands appeared at the same wavenumbers. These data demonstrate that the substituents on the bridging ligand do not affect the electron density on the Rh or Pd centers of the related complexes.

Reactivity Study. We previously demonstrated the selective photocatalytic dimerization of α-methylstyrene by the Ru···Pd dinuclear complex **9** (eq 1).[4] A reaction mechanism proposed for the catalytic dimerization is outlined in Scheme 3. The reaction sequence consists of two processes, i.e., the initial hydride formation step and the subsequent catalytic cycle. The first process involves insertion of α-methylstyrene (**12**) into the Pd−CH_3 bond in **9** to form the intermediate **A**, and subsequent β elimination generates the hydride intermediate **B**, which is the active species in the catalytic reaction. In the second process, successive insertion of two molecules of **12** into **B** (**B** → **C** → **D**) followed by β-H elimination gives the dimer **13** and **B**. NMR experiments revealed that the rate-determining step of the catalytic dimerization is the second insertion step of **12** (**C** → [**C***]).[4,28] Although the exact effect of light has not been elucidated yet, it was concluded that the rate of insertion ([**C**] → **D**) was significantly accelerated by visible light.

(27) The Rh complexes are prepared in the reaction of **1**−**3** with $[(cod)_2Rh]$-BF_4 and a subsequent reaction with CO gas. All of the complexes have been fully characterized by NMR and IR spectroscopies. The synthetic procedure and NMR data are shown in the Supporting Information.
(28) Inagaki, A.; Edure, S.; Munetaka, A., unpublished results.

In order to estimate the substituent effect of the bipyrimidine ligand on the photocatalytic reaction or, in other words, to understand the substituent effects on the energy/electron transfer across the bridging ligand, we have examined the reactions using **9**−**11** as catalysts.

All of the reactions were carried out at room temperature in a nitromethane solution containing 2 mol % of the catalyst. The consumption rate of the monomer **12** is plotted in Figure 8. In the reaction catalyzed by **10**, the head-to-tail dimer **13** was obtained selectively, and the initial rate was slightly larger than that catalyzed by **9**. It is notable that the Br-substituted catalyst **11** showed a catalytic activity much higher than that of **9** or **10**. In the reaction catalyzed by **11**, not only dimer **13** but small amounts of trimers were formed.[29] As described previously, electron densities on the Rh centers in the rhodium carbonyl complexes were not affected by the substituents on the bridging ligands judging from the C−O stretching bands. From this point of view, the above drastic increase in the reaction rate does not originate from the electronical or sterical effect[30] of the ligand substituents on the Pd center but from an efficient intramolecular energy transfer from the ruthenium(II) polypyridyl moiety to the Pd center through the bridging ligand (**L3**).[31] From the relationship between the reaction rate and the LUMO energy level of the mononuclear complexes **1**−**3**, it can be concluded that an electron-withdrawing substituent lowers the LUMO energy level so as to promote the energy transfer from Ru to Pd.

Conclusion

Mononuclear Ru complexes with a series of substituted bipyrimidine ligands and the corresponding dinuclear Ru···Pd and Ru···Rh complexes have been synthesized and characterized. Investigation of the electrochemical and photophysical properties of the complexes revealed that these properties of the dinuclear complexes rely on those of the corresponding mononuclear complexes $[(bpy)_2Ru(\mathbf{L}_n)]^{2+}$. Judging from the IR stretching bands of the rhodium carbonyl complexes, substituents on the bipyrimidine ligand do not change the electron density of the second metal center. Large differences in the photoluminescent quantum efficiencies among the mononuclear Ru complexes with various bipyrimidine ligands were observed, and DFT calculations have been performed to understand the substituent effect. It has been shown that the bipyrimidine ligand with electron-donating groups destabilizes the bipyrimidine-centered unoccupied MO at a higher energy level than that of the bipyridine-centered MOs, while that with electron-withdrawing groups stabilizes the energy level, thus resulting in the different LUMO character in each mononuclear complex.

The reactivities of the Pd complexes **9**−**11** with bipyrimidine bridging ligands **L1**−**L3** were compared through the photocatalytic reaction with **12**. The Pd complex with electron-withdrawing Br substituents resulted in a prominent increase of the reaction rate. This can be explained by an efficient energy transfer from the light-absorbing Ru unit to the reactive Pd center through the bipyrimidine ligand with a lower LUMO energy level. Further investigation to search an efficient photocatalytic reaction is in progress in our laboratory.

Experimental Section

General Procedures. Standard Schlenk and vacuum-line techniques under a N_2 atmosphere were employed for the coupling reactions of chloropyrimidines. Anhydrous *N*,*N*-dimethylformamide was purchased from Sigma-Aldrich and degassed under reduced pressure prior to use. Acetone (molecular sieves), acetonitrile (P_2O_5), and nitromethane ($CaCl_2$) were treated with appropriate drying agents, distilled, and stored under N_2. α-Methylstyrene was washed three times with aqueous 10% NaOH and six times with H_2O, dried over $CaCl_2$, and distilled under vacuum. ^1H and ^{13}C NMR spectra (Chart 3) were recorded on JEOL EX-400, LA 500, and Bruker AC-200 spectrometers. Solvents for NMR measurements were dried over molecular sieves, degassed, and stored under N_2. IR, UV−vis, and steady-state emission spectra were obtained on Jasco FT/IR 5300, Jasco V-570, and Shimadzu RF-5300PC spectrometers, respectively. ESI-MS spectra were recorded on a ThermoQuest Finnigan LCQ Duo mass spectrometer. Gas chromatography (GC) and GC−MS spectra were recorded on a Shimadzu GC-17A spectrometer and a Shimadzu QP-5000 mass spectrometer, respectively. Electrochemical measurements were made with a BAS CV-50W analyzer. $[(bpy)_2Ru(\mathbf{L1})](PF_6)_2$[17a] was prepared according to the published method. Other chemicals were purchased and used as received.

Chart 3. NMR Labels of Mono- and Dinuclear Ru^{II} Complexes with 2,2′-Bipyrimidine Ligands[a]

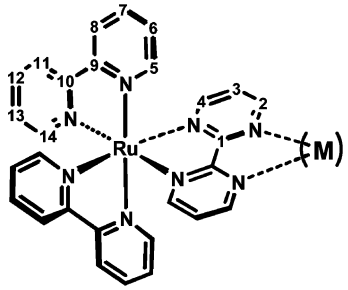

[a] Substituents on the bipyrimidine ligand are omitted for clarity.

Preparation of Bipyrimidines. 2,2′-Bipyrimidine (**L1**),[32] 5,5′-dibromo-2,2′-bipyrimidine (**L3**),[32] and 4,4′-dimethyl-2,2′-bipyrimidine (**L4**)[33] were prepared according to the published methods. 5,5′-Dimethyl-2,2′-bipyrimidine (**L2**) was prepared by a Ni^0-promoted coupling reaction[34] of 2-chloro-5-methylpyrimidine[35] (eq 2). Synthesis of 4,4′,6,6′-tetramethyl-2,2′-bipyrimidine (**L5**) by

(29) The products were analyzed by GC−MS spectra.
(30) X-ray diffraction studies clarified that substituents on the 5 and 5′ positions did not cause substantial sterical hinderance on both Ru and Pd centers.
(31) The observed similar reaction rates of **9** and **10** are probably due to the longer lifetimes of the excited species formed from **10** in comparison with **9** ($t\{[\mathbf{C}^{10}]^*\} > t\{[\mathbf{C}^{9}]^*\}$).
(32) Schwab, P. F. H.; Fleischer, F.; Michl, J. *J. Org. Chem.* **2002**, *67*, 443.
(33) Mukkala, V.-M.; Sund, C.; Kwiatkowski, M.; Pasanen, P.; Högberg, M.; Kankare, J.; Takalo, H. *Helv. Chem. Acta* **1992**, *75*, 1621.
(34) (a) Tiecco, M.; Testaferri, L.; Tingoli, M.; Chianelli, D.; Montanucci, M. *Synthesis* **1984**, 736. (b) Semelhack, M. F.; Helquist, P. M.; Jones, L. D. *J. Am. Chem. Soc.* **1971**, *93*, 5908.
(35) Synthesis of 2-chloro-5-methylpyrimidine: Hannout, I. B.; Johnson, A. *Dyes Pigm.* **1982**, *3*, 173.

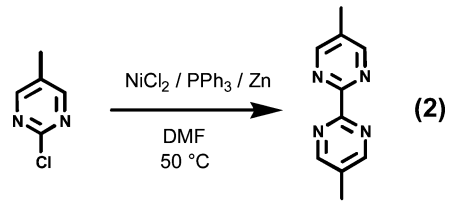

(2)

L2

Ullmann coupling was reported by Horváth and Vlád,[36] but we prepared it by a Ni^0 coupling reaction of 4,6-dimethyl-2-chloropyrimidine, which was synthesized from chlorination of 4,6-dimethyl-2-hydroxypyrimidine.[36]

L2. ^{1}H NMR (200 MHz, $CDCl_3$, RT, δ/ppm): δ 8.81 (s, 4H, H4, H4′, H6, H6′), 2.42 (s, 6H, $-CH_3$). ^{13}C NMR (100 MHz, $CDCl_3$, RT, δ/ppm): δ 159.8 (s, C^1), 157.7 (d, J_{CH} = 182.3 Hz, C^2, C^4), 130.8 (s, C^3), 15.5 (q, J_{CH} = 128.0 Hz, $-CH_3$).

Preparation of [(bpy)$_2$Ru(L2)](BF$_4$)$_2$ (2; L2 = 5,5′-Dimethyl-2,2′-bipyrimidine). *cis*-(bpy)$_2$RuCl$_2$·2H$_2$O (1.54 g, 2.96 mmol) and **L2** (0.78 g, 4.17 mmol) were suspended in EtOH−H$_2$O (90:10) and heated under N_2 at 50 °C for 5 h and at 110 °C for 10 h. The solvent was evaporated to dryness, and the resulting solid was dissolved in CH_3CN and stirred with excess NH_4BF_4. The complex was purified by column chromatography packed with neutral aluminum oxide (CH_3CN:CH_2Cl_2 = 1:4). Red crystals were obtained by diffusion of Et_2O into CH_3CN (2.24 g, 2.90 mmol, 98.0%). ESI-MS: *m*/*z* 687 [M − BF_4]$^+$, 860 [M + BF_4]$^-$. Anal. Calcd for $C_{30}H_{26}N_8RuB_2F_8$ (**2**·BF_4): C, 46.60; H, 3.39; N, 14.49. Found: C, 46.72; H, 3.39; N, 14.21. ^{1}H NMR (400 MHz, CD_3CN, RT, δ/ppm): δ 8.89 (d, J = 2.4 Hz, 2H, H^2), 8.52 (d, J = 7.9 Hz, 2H, H^8 or H^{11}), 8.50 (d, J = 7.6 Hz, 2H, H^8 or H^{11}), 8.09 (dd, J = 7.9 and 7.5 Hz, 2H, H^7, H^{12}), 8.06 (dd, J = 7.6 and 7.5 Hz, 2H, H^7 or H^{12}), 7.86 (d, J = 5.8 Hz, 2H, H^5 or H^{14}), 7.82 (d, J = 2.4 Hz, 2H, H^4), 7.66 (d, J = 5.8 Hz, 2H, H^5 or H^{14}), 7.43 (dd, J = 7.5 and 5.8 Hz, 2H, H^6 or H^{13}), 7.39 (dd, J = 7.5 and 5.8 Hz, 2H, H^6 or H^{13}), 2.24 (s, 6H, $-CH_3$). ^{13}C NMR (100 MHz, CD_3CN, RT, δ/ppm): δ 161.4 (s, C^1), 159.9 (d, J_{CH} = 186.4 Hz, C^4), 159.4 (d, J_{CH} = 186.4 Hz, C^2), 158.0 (s, C^9, C^{10}), 153.1 (d, J_{CH} = 192.2 Hz, C^5 or C^{14}), 152.7 (d, J_{CH} = 187.2 Hz, C^5 or C^{14}), 139.6 (d, J_{CH} = 169.0 Hz, C^7 or C^{12}), 139.0 (d, J_{CH} = 169.0 Hz, C^7 or C^{12}), 136.2 (s, C^3), 128.6 (d, J_{CH} = 170.6 Hz, C^6, C^{13}), 125.4 (d, J_{CH} = 167.3 Hz, C^8, C^{11}), 16.0 (q, J_{CH} = 129.2 Hz, $-CH_3$).

Preparation of [(bpy)$_2$Ru(L3)](BF$_4$)$_2$ (3; L3 = 5,5′-Dibromo-2,2′-bipyrimidine). The procedure used for the synthesis of **1** was applied (58.1%). ESI-MS: *m*/*z* 817 [M − BF_4]$^+$. Anal. Calcd for $C_{28}H_{20}Br_2N_8RuB_2F_8$: C, 37.24; H, 2.23; N, 12.41. Found: C, 36.85; H, 2.41; N, 12.77. ^{1}H NMR (400 MHz, CD_3CN, RT, δ/ppm): δ 9.16 (d, J = 2.4 Hz, 2H, H^2), 8.50 (d, J = 8.3 Hz, 2H, H^8 or H^{11}), 8.48 (d, J = 8.8 Hz, 2H, H^8 or H^{11}), 8.12 (dd, J = 8.3 and 7.6 Hz, 2H, H^7 or H^{12}), 8.09 (d, J = 2.4 Hz, 2H, H^4), 8.06 (dd, J = 8.8 and 7.4 Hz, 2H, H^7 or H^{12}), 7.59 (d, J = 5.9 Hz, 2H, H^5 or H^{14}), 7.59 (d, J = 5.8 Hz, 2H, H^5 or H^{14}), 7.46 (dd, J = 7.6 and 5.9 Hz, 2H, H^6 or H^{13}), 7.39 (dd, J = 7.4 and 5.8 Hz, 2H, H^6 or H^{13}). ^{13}C NMR (100 MHz, CD_3CN, RT, δ/ppm): δ 162.1 (s, C^1), 161.0 (d, J_{CH} = 190.5 Hz, C^4), 160.0 (d, J_{CH} = 196.3 Hz, C^2), 157.8 (s, C^9 or C^{10}), 157.7 (s, C^9 or C^{10}), 153.7 (d, J_{CH} = 186.4 Hz, C^5 or C^{14}), 152.9 (d, J_{CH} = 193.0 Hz, C^5 or C^{14}), 139.6 (d, J_{CH} = 169.8 Hz, C^7 or C^{12}), 139.5 (d, J_{CH} = 169.8 Hz, C^7 or C^{12}), 128.8 (d, J_{CH} = 176.4 Hz, C^6 or C^{13}), 128.7 (d, J_{CH} = 176.4 Hz, C^6 or C^{13}), 125.6 (d, J_{CH} = 162.3 Hz, C^8 or C^{11}), 125.5 (d, J_{CH} = 162.3 Hz, C^8 or C^{11}), 123.9 (s, C^3).

(36) Horváth, I. T.; Vlád, G. *J. Org. Chem.* **2002**, *67*, 6550.

Preparation of [(bpy)$_2$Ru(L4^A)](X)$_2$ (4A; X = PF$_6$, BF$_4$, L4^A = 4,4′-Dimethyl-2,2′-bipyrimidine). *cis*-(bpy)$_2$RuCl$_2$·2H$_2$O (393 mg, 0.755 mmol) and 4,4′-dimethyl-2,2′-bipyrimidine (198 mg, 1.06 mmol) were suspended in 30 mL of EtOH−H$_2$O (90:10), and the mixture was refluxed for 7 h. After the solution was evaporated to dryness, the resulting solid was dissolved in 20 mL of CH_3CN and then stirred for 2 h with $CuCl_2$·2H$_2$O (148 mg, 0.870 mmol) and excess NH_4BF_4. The reaction mixture was evaporated to dryness and subjected to purification by column chromatography packed with neutral aluminum oxide (CH_3CN:CH_2Cl_2 = 3:2). The eluted red band was collected, and the solvent was removed under vacuum. The obtained red solid was redissolved in CH_3CN, and slow diffusion of Et_2O into the solution yielded **4A** (X = BF_4) (109 mg, 0.122 mmol, 16.2%). In the synthesis of [(bpy)$_2$Ru(**L4^A**)](PF$_6$)$_2$, NH_4PF_6 was used in place of NH_4BF_4. This sample was used for the elemental analysis. ESI-MS (**4A**, X = BF_4): *m*/*z* 687 [M − BF_4]$^+$, 860 [M + BF_4]$^-$. Anal. Calcd for $C_{30}H_{26}N_8RuP_2F_{12}$ (X = PF_6): C, 40.50; H, 2.95; N, 12.60. Found: C, 40.35; H, 2.90; N, 12.44. ^{1}H NMR (data of **4A**, X = BF_4; 400 MHz, CD_3CN, RT, δ/ppm): δ 8.49 (d, J = 7.9 Hz, 2H, H^8 or H^{11}), 8.48 (d, J = 7.9 Hz, 2H, H^8 or H^{11}), 8.08 (dd, J = 7.9 and 7.4 Hz, 2H, H^7 or H^{12}), 8.05 (dd, obscure, 2H, H^7 or H^{12}), 7.88 (d, J = 5.9 Hz, 2H, H^5 or H^{14}), 7.81 (d, J = 5.9 Hz, 2H, H^4), 7.70 (d, J = 5.9 Hz, 2H, H^5 or H^{14}), 7.43 (dd, J = 7.4 and 5.9 Hz, 2H, H^6 or H^{13}), 7.40 (dd, J = 7.4 and 5.9 Hz, 2H, H_6 or H^{13}), 7.38 (d, J = 5.9 Hz, 2H, H^3), 2.72 (s, 6H, $-CH_3$). ^{13}C NMR (data of **4A**, X = BF_4; 100 MHz, CD_3CN, RT, δ/ppm): δ 170.8 (s, C^1), 163.4 (s, C^2), 159.0 (d, J_{CH} = 186.4 Hz, C^4), 158.0 (s, C^9 or C^{10}), 157.8 (s, C^9 or C^{10}), 153.1 (d, J_{CH} = 185.2 Hz, C^5 or C^{14}), 152.8 (d, J_{CH} = 182.7 Hz, C^5 or C^{14}), 139.1 (d, J_{CH} = 168.3 Hz, C^7 or C^{12}), 139.0 (d, J_{CH} = 168.3 Hz, C^7 or C^{12}), 128.7 (d, J_{CH} = 169.9 Hz, C^6 or C^{13}), 128.6 (d, J_{CH} = 169.9 Hz, C^6 or C^{13}), 125.3 (d, J_{CH} = 168.3 Hz, C^8, C^{11}), 124.9 (d, J_{CH} = 171.6 Hz, C^3), 24.6 (q, J_{CH} = 128.1 Hz, $-CH_3$).

Preparation of [(bpy)$_2$Ru(L5)](PF$_6$)$_2$ (5; L5 = 4,4′,6,6′-Tetramethyl-2,2′-bipyrimidine). *cis*-(bpy)$_2$RuCl$_2$·2H$_2$O (305.5 mg, 0.59 mmol), **L5** (148.7 mg, 0.69 mmol), and AgOTf (328.2 mg, 1.28 mmol) were charged into a flask, evacuated, put under N_2, and then dissolved in 40 mL of EtOH−H$_2$O (90:10). The solution was refluxed under N_2 for 20 h. The reaction mixture was evaporated to dryness, and the solid was dissolved in a minimum amount of H_2O. The solid was precipitated by the addition of a saturated aqueous solution of KPF_6. The precipitate was collected and washed by H_2O and Et_2O. The obtained solid was dissolved in a minimum amount of CH_3CN and reprecipitated by the addition of Et_2O. Red crystals were obtained via crystallization from CH_3CN−Et_2O (200 mg, 0.22 mmol, 37.1%). ESI-MS: *m*/*z* 773 [M − PF_6]$^+$, 1063 [M + PF_6]$^-$. Anal. Calcd for $C_{32}H_{30}N_8RuP_2F_{12}$: C, 41.88; H, 3.30; N, 12.21. Found: C, 41.68; H, 3.21; N, 12.04. ^{1}H NMR (400 MHz, CD_3CN, RT, δ/ppm): δ 8.51 (d, J = 8.1 Hz, 2H, H^8 or H^{11}), 8.42 (d, J = 8.1 Hz, 2H, H^8 or H^{11}), 8.13 (dd, J = 8.1 and 7.5 Hz, 2H, H^7 or H^{12}), 7.98 (d, J = 5.8 Hz, 2H, H^5 or H^{14}), 7.97 (dd, J = 8.1 and 7.4 Hz, 2H, H^7 or H^{12}), 7.63 (d, J = 5.8 Hz, 2H, H^5 or H^{14}), 7.51 (dd, J = 7.5 and 5.8 Hz, 2H, H^6 or H^{13}), 7.30 (s, 2H, H^3), 7.25 (dd, J = 7.4 and 5.8 Hz, 2H, H^6 or H^{13}), 2.64 (s, 6H, $-C^2H_3$), 1.62 (s, 6H, $-C^4H_3$). ^{13}C NMR (100 MHz, CD_3CN, RT, δ/ppm): δ 173.6 (s, C^4), 169.7 (s, C^2), 164.7 (s, C^1), 158.4 (s, C^9, C^{10}), 153.8 (d, J_{CH} = 183.9 Hz, C^5 or C^{14}), 152.9 (d, J_{CH} = 183.0 Hz, C^5 or C^{14}), 139.1 (d, J_{CH} = 169.8 Hz, C^7, C^{12}), 128.7 (d, J_{CH} = 170.6 Hz, C^6 or C^{13}), 128.5 (d, J_{CH} = 170.6 Hz, C^6 or C^{13}), 125.7 (d, J_{CH} = 168.1 Hz, C^8 or C^{11}), 125.5 (d, J_{CH} = 168.1 Hz, C^8 or C^{11}), 125.1 (d, J_{CH} = 170.6 Hz, C^3), 24.6 (q, J_{CH} = 129.2 Hz, $-CH_3$).

Preparation of $[(bpy)_2Ru(L1)Pd(Me)Cl](PF_6)_2$ (6). 1 (300 mg, 0.35 mmol) and (cod)PdMeCl (110 mg, 0.42 mmol) were dissolved in 15 mL of CH_3NO_2 and stirred for 3 h at ambient temperature. The solvent was removed under reduced pressure. The resulting solid was washed with Et_2O, dissolved in 1 mL of CH_3NO_2, and then precipitated with Et_2O. Reddish-brown crystals were obtained (346 mg, 0.34 mmol, 97.3%). ESI-MS : *m*/*z* 873 $[M - PF_6]^+$, 1163 $[M + PF_6]^-$. Anal. Calcd for $C_{29}H_{25}ClF_{12}N_8P_2PdRu$: C, 34.20; H, 2.47; N, 11.00. Found: C, 34.13; H, 2.74; N, 10.89. ^{1}H NMR (200 MHz, acetone-d_6, RT, δ/ppm): δ 9.17 (dd, J = 5.1 and 1.8 Hz, 1H, bpm), 9.14 (dd, J = 5.5 and 1.6 Hz, 1H, bpm), 8.84, (d, J = 7.8 Hz, 4H, bpy), 8.76 (dd, J = 5.7 and 1.6 Hz, 1H, bpm), 8.72 (dd, J = 5.7 and 1.6 Hz, 1H, bpm), 8.52 (m, 2H, bpy), 8.2−8.3 (m, 4H, bpy), 8.0−8.1 (m, 4H, bpy, bpm), 7.62 (dd, J = 7.2 and 6.1 Hz, 4H, bpy), 1.06 (s, 3H, PdC*H*$_3$). ^{13}C NMR (100 MHz, CD_3NO_2, RT, δ/ppm): δ 167.5 (s, bpm), 165.4 (s, bpm), 162.4 (d, J_{CH} = 191.7 Hz, bpm), 161.9 (d, J_{CH} = 192.6 Hz, bpm), 158.9 (s, bpy), 158.6 (s, bpy), 156.7 (d, J_{CH} = 196.3 Hz, bpm), 156.5 (d, J_{CH} = 181.8 Hz, bpm), 154.6 (d, J_{CH} = 176.4 Hz, bpy), 153.7 (d, J_{CH} = 183.9 Hz, bpy), 153.6 (d, J_{CH} = 183.9 Hz, bpy), 140.7 (d, J_{CH} = 169.8 Hz, bpy), 140.6 (d, J_{CH} = 169.8 Hz, bpy), 129.6 Hz, (d, J_{CH} = 171.4 Hz, bpy), 128.2 (d, J_{CH} = 142.0 Hz, bpm), 128.0 (d, J_{CH} = 144.9 Hz, bpm), 126.7 (d, J_{CH} = 171.4 Hz, bpy), 126.3 (d, J_{CH} = 167.7 Hz, bpy), −0.49 (q, J_{CH} = 135.1 Hz, Pd−CH_3).

Preparation of $[(bpy)_2Ru(L2)Pd(Me)Cl](BF_4)_2$ (7). The procedure used for the synthesis of **6** was applied (80.9%). ESI-MS: *m*/*z* 843 $[M - BF_4]^+$, 1017 $[M + BF_4]^-$. Anal. Calcd for $C_{31}H_{29}B_2ClF_8N_8PdRu$: C, 40.03; H, 3.14; N, 12.05. Found: C, 40.00; H, 3.21; N, 12.02. ^{1}H NMR (400 MHz, CD_3CN, RT, δ/ppm): δ 8.82, 8.75 (2H, s, H^2), 8.55, 8.53 (d, J = 9.0 Hz, 4H, H^8, H^{11}), 8.14, 8.07 (dd, J = 8.0 and 7.3 Hz, 4H, H^7, H^{12}), 8.05 (b d, 2H, H^5 or H^{14}), 8.00 (s, 2H, H^4), 7.64 (d, J = 5.4 Hz, 2H, H^5 or H^{14}), 7.52, 7.42 (dd, J = 6.5 and 6.2 Hz, 4H, H^6, H^{13}), 2.36 (s, 6H, bpm−CH_3), 0.94 (s, 3H, Pd−CH_3). ^{13}C NMR (100 MHz, CD_3CN, RT, δ/ppm): δ 161.2 (b s, C^1, C^2), 158.0, 157.7 (s, C^9, C^{10}), 155.8 (b d, C^4), 154.3, 152.9 (d, J_{CH} = 182.3 and 185.6 Hz, C^5, C^{14}), 139.5, 139.4 (d, J_{CH} = 167.5 Hz, C^7, C^{12}), 139.2 (s, C^3), 128.8 (d, J_{CH} = 161.7 Hz, C^6, C^{13}), 125.5 (d, J_{CH} = 166.6 Hz, C^8, C^{11}), 16.6 (q, J_{CH} = 129.0 Hz, bpm−CH_3), −1.0 (q, J_{CH} = 134.5 Hz, Pd−CH_3).

Preparation of $[(bpy)_2Ru(L3)Pd(Me)Cl](BF_4)_2$ (8). Complex **3** (349.2 mg, 0.387 mmol) and [(cod)Pd(CH_3)(Cl)] (123.1 mg, 0.464 mmol) were dissolved in 10 mL of CH_3NO_2, and the solution was stirred for 4 h. Removal of the solvent under reduced pressure gave a black solid. Recrystallization from Me_2CO−Et_2O gave **8** as a black crystalline solid (349.7 mg, 0.330 mmol, 85.3%). ESI-MS: *m*/*z* 973 $[M - BF_4]^+$. Anal. Calcd for $C_{29}H_{23}B_2Br_2ClF_8N_8PdRu$: C, 32.86; H, 2.19; N, 10.57. Found: C, 32.26; H, 2.73; N, 10.54. ^{1}H NMR (400 MHz, CD_3CN, 313 K, δ/ppm): δ 9.13 (b s, 2H, H^2), 8.52, 8.51 (m, 4H, H^8, H^{11}), 8.16 (m, 2H, H^5 or H^{14}), 8.15, 8.07 (m, 4H, H^7, H^{12}), 7.95 (b s, 2H, H^4), 7.81 (m, 2H, H^5 or H^{14}), 7.51, 7.41 (m, 4H, H^6, H^{13}), 0.95 (b s, 3H, Pd−CH_3). ^{13}C NMR (125 MHz, CD_3CN, 243 K, δ/ppm): δ 162.8 (s, C^1), 161.0 (d, J_{CH} = 191.1 Hz, C^4), 159.7 (d, J_{CH} = 196.4 Hz, C^2), 157.5 (s, C^9, C^{10}), 153.6 (d, J_{CH} = 186.1 Hz, C^5 or C^{14}), 152.9 (d, J_{CH} = 187.1 Hz, C^{14} or C^5), 139.6 (d, J_{CH} = 169.5 Hz, C^7 or C^{12}), 139.2 (d, J_{CH} = 169.5 Hz, C^{12} or C^7), 128.4 (d, J_{CH} = 169.5 Hz, C^6, C^{13}), 125.3 (d, J_{CH} = 167.5 Hz, C^8 or C^{11}), 125.2 (d, J_{CH} = 167.5 Hz, C^{11} or C^8), 123.7 (s, C^3), 0.0 (q, J_{CH} = 135.3 Hz, Pd−CH_3).

Preparation of $[(bpy)_2Ru(L1)Pd(Me)(Me_2CO)](PF_6)_2(BF_4)$ (9). **6** (325 mg, 0.32 mmol) and $AgBF_4$ (140 mg, 0.72 mmol) were dissolved in 7 mL of Me_2CO and stirred for 1 h at room temperature. The solution was filtered and then concentrated. A brown solid was obtained after precipitation with 20 mL of Et_2O. The solid was washed with Et_2O and then dichloromethane and dried in vacuo. Reddish-brown crystals were grown by diffusion of Et_2O into a Me_2CO solution (329 mg, 0.29 mmol, 91.3%). ESI-MS : *m*/*z* 1098 $[M - 2PF_6 + 3BF_4]^-$, 1156 $[M - PF_6 + 2BF_4]^-$, 1214 $[M + BF_4]^-$, 1273 $[M + PF_6]^-$. Anal. Calcd for $C_{32}H_{31}BF_{16}N_8OP_2PdRu$: C, 34.08; H, 2.77; N, 9.94. Found: C, 34.52; H, 3.18; N, 9.48. ^{1}H NMR (200 MHz, CD_3NO_2, RT, δ/ppm): δ 8.94 (m, 1H, bpm), 8.74 (m, 1H, bpm), 8.59 (d, J = 8.2 Hz, 4H, bpy), 8.46 (d, J = 5.5 Hz, 2H, bpm), 8.07−8.24 (m, 6H, bpm (2H), bpy (4H)), 7.80−7.85 (m, 4H, bpy), 7.44−7.58 (m, 4H, bpy), 2.23 (b s, 6H, Me_2CO), 1.30 (s, 3H, Pd−CH_3). ^{13}C NMR (100 MHz, CD_3NO_2, RT, δ/ppm): δ 167.1 (s, bpm) 164.4 (s, bpm), 162.6 (d, J_{CH} = 194.0 Hz, bpm), 162.3 (d, J_{CH} = 194.0 Hz, bpm), 158.3 (s, bpy), 158.1 (s, bpy), 157.5 (d, J_{CH} = 197.0 Hz, bpm), 156.4 (d, J_{CH} = 197.0 Hz, bpm), 154.0 (d, J_{CH} = 183.1 Hz, bpy), 153.1 (d, J_{CH} = 183.1 Hz, bpy), 140.4 (dd, J_{CH} = 164.2 and 6.6 Hz, bpy) 140.2 (dd, J_{CH} = 164.2 and 6.6 Hz, bpy), 129.4 (dd, J_{CH} = 170.8 and 7.3 Hz, bpy), 129.2 (dd, J_{CH} = 170.8 and 7.3 Hz, bpy), 128.1 (d, J_{CH} = 177.7 Hz, bpm), 127.8 (d, J_{CH} = 177.7 Hz, bpm), 125.8 (dd, J_{CH} = 167.5 and 7.5 Hz, bpy), 32.0 (q, J_{CH} = 127.0 Hz, *Me*$_2$CO), 5.2 (q, J_{CH} = 137.0 Hz, Pd−*Me*). A signal attributable to the quaternary C atom of the acetone ligand was not observed in the ^{13}C NMR spectrum in the temperature range of +25 to −30 °C.

Preparation of $[(bpy)_2Ru(L2)Pd(Me)(Me_2CO)](BF_4)_3$ (10). The procedure used for the synthesis of **9** was applied (97.5%). ESI-MS: *m*/*z* 953 $[M - BF_4]^+$, 1068 $[M - Me_2CO + BF_4]^-$. Anal. Calcd for $C_{34}H_{35}B_3F_{12}N_8OPdRu$: C, 39.28; H, 3.39; N, 10.78. Found: C, 39.10; H, 3.43; N, 10.58. ^{1}H NMR (400 MHz, CD_3CN, RT, δ/ppm): δ 8.91, 8.85 (b s, 2H, H^2), 8.59, 8.57 (m, 4H, H^8, H^{11}), 8.29, 8.27 (s, 2H, H^4), 8.20, 8.12 (t, J = 7.9 Hz, 4H, H^7, H^{12}), 8.08 (m, 2H, H^5 or H^{14}), 7.81 (m, 2H, H^5 or H^{14}), 7.56, 7.45 (t, 4H, J = 6.7 Hz, H^6, H^{13}), 2.36, 2.33 (s, 6H, bpm−CH_3), 2.27 (b s, *Me*$_2$CO), 1.38 (b s, 3H, Pd−CH_3). ^{13}C NMR (100 MHz, CD_3CN, RT, δ/ppm): δ 164.3 (s, C^1) 162.0, 161.7 (b d, C^2), 158.4, 158.2 (s, C^9, C^{10}), 156.3 (b d, C^4), 154.0, 153.1 (d, J_{CH} = 183.2 and 180.7 Hz, C^5, C^{14}), 140.1 (s, C^3), 140.1, 140.0 (d, J_{CH} = 169.1 and 162.5 Hz, C^7, C^{12}), 129.2, 129.1 (d, J_{CH} = 165.0 and 169.9 Hz, C^6, C^{13}), 125.7 (d, J_{CH} = 167.1 Hz, C^8, C^{11}), 31.7 (q, J_{CH} = 126.2 Hz, *Me*$_2$CO), 16.6 (q, J_{CH} = 132.0 Hz, bpm−CH_3), 5.5 (q, J_{CH} = 145.2 Hz, Pd−CH_3). A signal attributable to the quaternary C atom of the acetone ligand was not observed in the ^{13}C NMR spectrum in the temperature range of +25 to −30 °C.

Preparation of $[(bpy)_2Ru(L3)Pd(Me)(Me_2CO)](BF_4)_3$ (11). The procedure used for the synthesis of **9** was applied (76.0%). ESI-MS: *m*/*z* 1197 $[M - Me_2CO + BF_4]^-$. Anal. Calcd for $C_{32}H_{29}B_3Br_2F_{12}N_8OPdRu$: C, 32.87; H, 2.50; N, 9.58. Found: C, 32.23; H, 3.13; N, 9.64. ^{1}H NMR (400 MHz, CD_3CN, RT, δ/ppm): δ 9.16 (b s, 2H, H^2), 8.53 (t, J = 9.2 Hz, 4H, H^8, H^{11}), 8.15 (t, J = 7.3 Hz, 2H, H^{7}or H^{12}), 8.13 (b s, 2H, H^4), 8.08 (td, J = 7.9 and 1.5 Hz, 2H, H^7 or H^{12}), 7.94 (d, J = 5.1 Hz, 2H, H^5 or H^4), 7.62 (d, J = 5.1 Hz, 2H, H^5 or H^{14}), 7.50 (t, J = 6.3 Hz, 2H, H^6 or H^{13}), 7.42 (ddd, J = 6.6, 5.6, and 1.6 Hz, 2H, H^6 or H^{13}), 1.09 (b s, 3H, Pd−CH_3). ^{13}C NMR (125 MHz, CD_3CN, 243 K, δ/ppm): δ 161.3 (s, C^1), 160.8 (d, J_{CH} = 194.3 Hz, C^4), 159.4 (d, J_{CH} = 196.4 Hz, C^2), 157.1 (s, C^9, C^{10}), 153.3 (d, J_{CH} = 186.0, C^5, C^{14}), 152.5 (d, J_{CH} = 181.9 Hz, C^5, C^{14}), 138.9 (d, J_{CH} = 168.5 Hz, C^7, C^{12}), 128.2 (d, J_{CH} = 170.5 Hz, C^6 or C^{13}), 128.0 (d, J_{CH} = 170.5 Hz, C^{13} or C^6), 124.9 (d, J_{CH} = 167.4 Hz, C^8, C^{11}), 123.4 (s, C^3), −3.7 (q, J_{CH} = 140.5 Hz, Pd−CH_3). A signal attributable to the quaternary C atom of the acetone ligand was not

observed in the ^{13}C NMR spectrum in the temperature range of +25 to −30 °C.

Electrochemical Measurements. CV measurements were performed with a Pt electrode for CH_3CN solutions of the samples (ca. 2×10^{-3} M) in the presence of an electrolyte (0.1 M $Bu_4N \cdot BF_4$) at ambient temperature under an inert atmosphere. The scan rates were 100 mV s^{-1}. After the measurements, ferrocene (Fc) was added to the mixture and the potentials were calibrated with respect to the Fc/Fc^+ redox couple.

DFT Calculations. DFT calculations were performed using the *Gaussian 03* quantum chemistry program package at the B3LYP/LanL2DZ level. The HOMO and LUMO energies were determined by using minimized singlet geometries to approximate the ground state.

Crystal Structure Determination. The crystallographic data and the results of the structure refinements are summarized in Table 1. In the reduction of data, Lorentz and polarization corrections and empirical absorption corrections were made.[37] The structures were solved by a combination of the direct methods (*SHELXS-86*)[38] and Fourier synthesis (*DIRDIF94*).[39] Unless otherwise stated, all non-H atoms were refined anisotropically, methyl H atoms were refined using riding models, and other H atoms were fixed at the calculated positions. **2**: Three sets of disordered F atoms on two BF_4 anions were refined isotropically, taking into account three components (occupancies were fixed at 0.3333 for all of the F atoms). **3**: Three sets of disordered F atoms on one BF_4 anion were refined isotropically, taking into account three components with occupancies for the F atoms fixed at 0.3333. Three independent BF_4 anions were included in the single crystal, although **3** was a dicationic complex. It might be possible that Br was protonated (H1A) to have a BF_4 anion as its counterion. **4**: Three sets of disordered F atoms on one $P(1)F_6$ anion and two sets of disordered F atoms on $P(2)F_6$ anions were refined isotropically, taking into account three and two components, respectively (occupancies fixed at 0.3333 for F on P^1 and 0.50 on P^2). The Me_2CO solvate molecule was refined isotropically, taking into account two components (occupancies were fixed at C33:C33a = 0.50:0.50), and the H atoms attached to the solvate molecule were not included in the refinement. All of the H atoms except methyl H atoms on the bipyrimidine ligand and H22 were located by difference Fourier synthesis. **5**: Three sets of F atoms on two PF_6 anions were refined isotropically, taking into account three components (occupancies were fixed at 0.3333 for all of the F atoms). **6**: One of the two solvate CH_3NO_2 molecules was disordered and refined isotropically, taking into account two components (C33:C33A = 73.6:26.7). H atoms attached to the disordered part were not included in the refinement.

Photochemical Reaction. Typical reaction procedures: To a CD_3NO_2 (or CH_3NO_2) solution (0.4 mL) of **9** (10 mg, 0.01 mmol) was added α-methylstyrene (0.5 mmol, s/c = 50) and cyclooctane (10.0 μL, as an internal standard). The solution was divided into two 5-mm-diameter glass tubes: one for the irradiation and the other for the dark reaction, in which the tube was foiled with an aluminum sheet. The two samples were placed at a distance of 10 cm from a Xe lamp [150 W, with a L42 cutoff filter (λ > 420 nm)]. The reaction was followed by ^1H NMR and/or GC after appropriate time intervals.

Acknowledgment. This research was financially supported by the Japan Society for Promotion of Science and Technology [Grant-in-Aid for Young Scientists (B) 16750046 and Grant-in-Aid for Scientific Research (B) 15350032] and the Ministry of Education, Culture, Sports, Science and Technology of the Japanese Government (Grant-in-Aid for Scientific Research on Priority Areas 18065009, "Chemistry of Concerto Catalysis"), which are gratefully acknowledged.

Supporting Information Available: Tables of crystal data, experimental procedures for X-ray crystallography, bond distances and angles for $[(bpy)_2Ru(\mathbf{L2})]^{2+}$ (**2**), $[(bpy)_2Ru(\mathbf{L3})]^{2+}$ (**3**), $[(bpy)_2Ru(\mathbf{L4})]^{2+}$ (**4**), $[(bpy)_2Ru(\mathbf{L5})]^{2+}$ (**5**), and $[(bpy)_2Ru(bpm)PdMeCl]^{2+}$ (**6**), Cartesian coordinates and absolute energies for all computed structures, preparation and spectroscopic data for dinuclear Ru···Rh carbonyl complexes $[(bpy)_2Ru(\mathbf{L})Rh(CO)_2]^{3+}$ (**L** = **L1**, **L2**, **L3**), CV spectra of **1**−**11**, UV−vis and emission spectra of **6**−**11**, NMR spectra of complexes **1**−**5**, **7**, **8**, **10**, and **11**, and X-ray crystallographic data in CIF format. This material is available free of charge via the Internet at http://pubs.acs.org.

IC0612909

(37) Higashi, T. *Program for absorption correction*; Rigaku Corp.: Tokyo, Japan, 1995.

(38) (a) Sheldrick, G. M. *SHELXS-86: Program for crystal structure determination*; University of Göttingen: Göttingen, Germany, 1986. (b) Sheldrick, G. M. *SHELXL-97: Program for crystal structure refinement*; University of Göttingen: Göttingen, Germany, 1997.

(39) Beurskens, P. T.; Admiraal, G.; Beurskens, G.; Bosman, W. P.; de Gelder, R.; Israel, R.; Smits, J. M. M. *DIRDIF99: The DIRDIF-99 program system*; Technical Report of the Crystallography Laboratory; University of Nijmegen: Nijmegen, The Netherlands, 1999.